



A multi-proxy analysis of late Quaternary Indian monsoon dynamics for the Maldives, Inner Sea

5 Dorothea Bunzel¹, Gerhard Schmiedl¹, Sebastian Lindhorst¹, Andreas Mackensen², Jesús Reolid¹, Sarah Romahn¹, Christian Betzler¹

¹Center for Earth System Research and Sustainability (CEN), Institute for Geology, University of Hamburg, Hamburg, D-20146, Germany

²Alfred Wegener Institute (AWI), Helmholtz Centre for Polar and Marine Research, Bremerhaven, D-27568, Germany

Correspondence to: Dorothea Bunzel (dorothea.bunzel@uni-hamburg.de)

10

Abstract. We present a detailed multi-proxy data record to reveal the late Quaternary changes in marine sedimentation and biogeochemical processes of the upper bathyal Maldives (equatorial Indian Ocean) and how they are related to the benthic ecosystem dynamics. We investigated the sediment core SO-236-052-4 from the central part of the Inner Sea, Maldives, focusing on Fe/Ca and Si/Ca ratios as proxies for terrigenous sediment delivery, as well as Total Organic Carbon (TOC) and Ba/Ca ratios as proxies for marine productivity. Benthic foraminiferal fauna distributions, sortable silt records and stable oxygen and carbon isotope analyses were used for reconstructing the past ecosystem, as well as changes in the intermediate water circulation, bottom water current velocity and oxygenation.

15

This multi-proxy data record shows an enhanced dust supply during the glacial intervals, represented by increased Fe/Ca and Si/Ca ratios, an overall coarsening of the sediment and increasing amount of agglutinated benthic foraminifera. The enhanced dust fluxes can be attributed to higher dust availability in the Asian desert and loess areas and its transport by intensified winter monsoon winds during glacial conditions. These combined effects of wind-induced mixing of surface waters and dust fertilisation during the cold phases resulted in increased surface water productivity and related organic carbon fluxes. Thus, the development of highly diverse benthic foraminiferal faunas and the distribution of certain detritus and suspension feeders were fostered.

20

The difference in the stable carbon isotope signal between epifaunal and deep infaunal benthic foraminifera reveals intermediate water oxygen concentrations between approximately 40 and 100 $\mu\text{mol kg}^{-1}$. The pattern of oxygen changes resembles that from the deep Arabian Sea suggesting an expansion of the Oxygen Minimum Zone (OMZ) from the Arabian Sea into the tropical Indian Ocean, further controlled by the inflow of the Antarctic Intermediate Water (AAIW). The precessional circulation pattern of the bottom water oxygenation is overprinted by glacial-/interglacial changes resulting in a long phase of reduced ventilation during the last glacial period. The latter process is likely linked to the combined effects of generally enhanced oxygen consumption rates during high-productivity phases, reduced AAIW production and restriction of bathyal environments of the Inner Sea of the Maldives during sea-level lowstands. Thus, this multi-proxy record provide a close linkage between the Indian monsoon oscillation, intermediate water circulation, productivity and sea-level changes on orbital time-scale.

30



35

1 Introduction

Sedimentation and biogeochemical processes of the tropical and subtropical northern Indian Ocean are closely linked to the intensity and seasonal changes of the Indian monsoon system. From June to October, the region is dominated by the SW monsoon, while the NE monsoon operates from December to April (Wyrski, 1973; Schott and McCreary, 2001). During the
40 SW monsoon, coastal and open-ocean upwelling in the Arabian Sea results in maximum surface water productivity and related organic matter fluxes (Nair et al., 1989, Rixen et al., 1996). At the same time, the Southwest Monsoon Current (SMC) transports high-saline surface waters from the Arabian Sea into the equatorial region (Schott and McCreary, 2001). During the NE monsoon, the current system reverses and the Northeast Monsoon Current (NMC) transports lower-saline surface waters from the Bay of Bengal into the western Indian Ocean. While chlorophyll concentrations strongly decrease in
45 the Arabian Sea during the NE monsoon, elevated concentrations are mainly restricted to the Indian west coast. In the Maldives area, mean chlorophyll concentrations reach their maximum during the NE monsoon (Sasamal, 2007; de Vos et al., 2014; NASA MODIS-Aqua, 2014).

The decay of organic matter in the water column and the generally reduced ventilation of regional subsurface waters in the Indian Ocean result in the development of a strong Oxygen Minimum Zone (OMZ) between 200 and 1200 m water depth
50 (Reid, 2003; Stramma et al., 2008). The oxygen depletion is fostered by the semi-enclosed nature of the northern Indian Ocean, the long pathway of intermediate water from its main formation sites at 40°S in the central South Indian Ocean (Antarctic Intermediate Water, AAIW) and Indonesia (Indonesian Intermediate Water, IIW) (Olson et al., 1993; You, 1998), and the contribution of low-oxygen outflow waters from the Red Sea and the Persian Gulf (Jung et al., 2001; Prasad and Ikeda, 2001). The OMZ extends from the Arabian Sea into the equatorial Indian Ocean. While oxygen concentrations in the
55 Arabian Sea can be as low as 0.1 ml l⁻¹ (or 5 μmol kg⁻¹) (Reid, 2003), they still reach low oxic values around 1 ml l⁻¹ (or 45 μmol kg⁻¹) in 500 to 1000 m water depths of the Maldives region (Weiss et al., 1983; Reid, 2003).

The evaluation of deep-sea sediment archives from the Arabian Sea delivered comprehensive information on the pacing and intensity of the Indian summer monsoon and response of deep-sea environments on orbital (Clemens and Prell, 1990; Clemens et al., 1991) and suborbital (Schulz et al., 1998; Gupta et al., 2003) time scales. Summer monsoon changes are
60 strongly coherent over the precessional band and reveal a close but lagged response to maxima in northern hemisphere summer insolation (Clemens and Prell, 2003). Phases of intensified OMZ are related to increased organic matter fluxes and microbial oxygen consumption rates during summer monsoon maxima (Den Dulk et al., 2000). In contrast, deep vertical mixing and erosion of the OMZ occurred during phases of intensified winter monsoon (Reichart et al., 1998). More recent studies revealed that the intensity of the OMZ and dynamics of deep-sea benthic ecosystems are paced by the superposition
65 of regional monsoon dynamics and super-regional changes of intermediate and deep-water ventilation (Schmiedl and Leuschner, 2005; Pattan and Pearce, 2009; Das et al., 2017).



Records from the equatorial Indian Ocean provide a more diverse and partly contradictory picture since this region is not only influenced by the summer and winter monsoons but also by the strength of Indian Ocean Equatorial Westerlies (IEW) which are strongest during the intermonsoon seasons in spring and fall and are inversely related to the Indian Ocean Dipole
70 (Hastenrath et al., 1993; Beaufort et al., 2001). Variations in surface water properties in the southeastern Arabian Sea at a site close to the Maldives platform revealed maximum productivity at times of enhanced winter monsoon winds associated with precessional maxima in ice volume (Rostek et al., 1997). An upper bathyal benthic foraminiferal record from the Maldives Ridge suggests that late Quaternary changes in organic matter fluxes are either driven by summer monsoon winds (Sarkar and Gupta, 2009) or linked to changes in the IEW strength (Sarkar and Gupta, 2014). The precessional variability in
75 productivity records from the equatorial Indo-Pacific Ocean has been attributed to the influence of low-latitude insolation on the IEW strength and on long-term dynamics of the El Niño-Southern Oscillation (ENSO) (Beaufort et al., 1997, 2001).

Here we present a multi-proxy data set on the links between climate variability, ocean circulation, sedimentation and biogeochemical processes of the Maldives Inner Sea. Specifically, our study addresses the following questions: (1) Which impact did orbital-scale changes of the Indian monsoon have on dust fluxes and marine environments of the Maldives? (2)
80 How did global sea-level changes influence the sedimentation processes and benthic ecosystems of the Maldives Inner Sea? (3) Can we trace the influence of changes in the configuration of intermediate waters and how are these changes related to super-regional oceanographic processes?

The sediment archive of the Maldives Inner Sea is ideally situated to answer the above questions because it lies in the central part of the Indian Ocean and therefore it is in the zone where the different processes introduce above acts. The
85 Maldives also appear as an ideal place to trace back paleoceanographic variations in time, as seismic surveys (Betzler et al. 2009, 2013a, 2013b, 2016; Lüdmann et al., 2013) have shown that the Maldives are comparable to a large natural sediment trap with a continuous Neogene succession.

2 Material and Methods

90 2.1 Sediment cores and material descriptions

For this study, two sediment cores were retrieved from different sites in the Inner Sea of the Maldives (Fig. 1). The 5.97 m long sediment core SO-236-052-4 was obtained by means of a gravity corer in the framework of R/V SONNE cruise SO236 in August 2014, E of the North Ari Atoll in the central part of the Inner Sea (03°55.09'N; 73°08.48'E) and from a water depth of 381.9 m. The 12.94 m long sediment core M74/4-1143 is a piston core from R/V METEOR cruise M74/4, obtained
95 in 2007 from E of the Goidhoo Atoll (04°49.50'N; 73°05.04'E) at a water depth of 386.8 m (Fig. 1). This study is focused on the first 6.00 m of core M74/4-1143.

The sediment of core SO-236-052-4 consists of an alternation of non-lithified fine-grained ooze with abundant pteropods, sponge spicules, planctonic and benthic foraminifera, and echinoid remains, with minor otolites and fragments of gastropods and bivalves. There are locally some intervals that present up to 4 cm bioclast including solitary corals and thin-shelled



100 bivalves. The entire succession is intensely reworked by bioturbation. Just a few primary structures, usually main boundaries
between facies are preserved (i.e. the sharp contacts at 2.35 mbsf and at 3.90 mbsf). Discrete burrows are scarce. The
succession recovered at site M74/4-1143 has been described by Betzler et al. (2013b). The core consists mainly of
periplatform ooze with planktic foraminifers, pteropods, otoliths, mollusc remains, benthic foraminifers, sponge spicules,
and echinoid debris. Down the core, light and dark colored greenish to olive gray intervals alternate, with the light colored
105 intervals correlating to isotopically lighter intervals and the darker colored intervals correlating to isotopically heavier
intervals (Betzler et al., 2013b).

2.2 Geochemical analyses

Scanning X-Ray Fluorescence (XRF) element analysis of core SO-236-052-4 was carried out at the MARUM, University of
110 Bremen, using an Avaatech XRF Core Scanner II. Element analysis was performed at 1 cm intervals, using generator
settings of 50 kV (1.0 mA current), 30 kV (1.0 mA) and 10 kV (0.2 mA), and a sampling time of 20 seconds per
measurement. Raw data spectra were processed using the software package WIN AXIL. Element ratios (Ba, Fe, Si, Sr
against Ca) were calculated and used for environmental interpretations following Croudace and Rothwell (2015).

The calcium carbonate and Total Organic Carbon (TOC) content of core SO-236-052-4 was measured at 5 cm spacing.
115 The carbon content of the grain-size fraction < 63 µm was determined using a LECO DR144 carbon analyser. All samples
were freeze dried. Subsequently, one subsample was measured at 1350 °C to obtain the total carbon content. A second
subsample was heated to 550 °C for 5 hours to remove the organic carbon prior to measurement in the LECO; this gave the
inorganic carbon content. The difference between total carbon- and inorganic carbon- is regarded as the organic-carbon
content. Calcium carbonate contents were calculated from the inorganic carbon content.

120

2.3 Grain-size analyses

For bulk grain size analysis core SO-236-052-4 was sampled equidistantly (1.5 cm³ each 1 cm). Samples were wet-sieved
(2000 µm) to remove very coarse particles, and subsequently suspended in water with addition of a 0.05 % solution of Tetra-
Sodium Diphosphate Decahydrate as dispersant.

125 The mean grain size of the non-carbonate fraction between 10 to 63 µm, the sortable silt, has been shown to be a reliable
proxy for palaeocurrent strength in predominantly siliciclastic sediments (Manighetti and McCave, 1995; McCave et al.,
1995a, 1995b; Hall et al., 1998; Bianchi et al., 1999; McCave and Hall, 2006). The method makes use of the non-carbonate
fraction only and is therefore expected to be unaffected by primary carbonate production and burial diagenesis. Samples for
the determination of the sortable silt component (c. 20 cm³ each) were taken equidistantly (at 5 cm intervals down to 1 m
130 below the sea floor and at 10 cm intervals underneath for core M74/4-1143 and at 5 cm downcore intervals for core SO-236-
052-4). Subsequently to wet-sieving, the fraction < 63µm was cooked in H₂O₂ to remove the organic portion, and treated



with 1M Ca₃COOH to dissolve the carbonate. Biogene opal was removed with 2M NaHCO₃. The remainder was dispersed in water for grain-size determination.

All grain-size measurements were done using a Helos KFMagic Laser particle size analyzer and measuring ranges of
135 either 0.5/18-3500 μm (for bulk grain size) or 0.25/87.5 μm (for the non-carbonate fraction). To ensure accuracy of measurements and absence of a long-term instrumental drift, an in-house grain-size standard was measured regularly. Grain size statistics are based on the graphical method (Folk and Ward, 1957) and were calculated using the software GRADISTAT (Blott and Pye, 2001).

140 2.4 Foraminiferal faunal and stable isotope analyses

For stable isotope analyses core SO-236-052-4 was sampled at 5 cm spacing and for benthic foraminiferal faunal analysis at 10 cm spacing. All Samples were wet-sieved over a 63 μm screen and the residues subsequently dried at 38 °C. The benthic foraminiferal analysis was carried out on the > 125 μm size fraction and based on allocate splits in order to obtain approximately 300 tests. Genus and species identifications mainly based on Loeblich and Tappan (1988), Hottinger et al.
145 (1993), Jones (1994), Debenay (2012), Milker and Schmiedl (2012) and Holbourn et al. (2013). The genera *Cymbaloporeta* and *Tretomphaloides* were summarized as meroplanktonic benthic foraminifera (BF) since they are known to have planktonic drift phases as part of their dispersal strategy (Banner et al., 1985; Alve, 1999). For analysis based on the test material all individuals of the foraminiferal orders Astrorhizida, Lituolida and Textulariida were summarized as agglutinated BF.

Benthic foraminiferal assemblages were defined by Q-mode Principal Component Analysis (PCA) with varimax rotation using the software SYSTAT, version 5.2.1. Following Schmiedl et al. (1997) only foraminiferal taxa with percentages ≥ 1 % in at least one sample and/or taxa, which occur at least in two samples were used for the statistical analysis. Loadings ≥ 0.5 were defined as significant (Backhaus et al., 2008). The Shannon-Wiener diversity index H(S) was calculated after Murray (2006) based on the function $H(S) = (-1) \sum_{i=1}^S p_i \times \ln(p_i)$, where S is the species number and p_i the relative abundance of
155 the i-th species.

Stable oxygen and carbon isotope records were generated for planktonic and benthic foraminifera. Approximately 10 tests of the planktonic foraminifer *Globigerinoides ruber* (white) were selected from the 250-350 μm size fraction of core SO-236-052-4. Stable isotope data of *G. ruber* (white) of core M74/4-1143 were taken from Betzler et al. (2013b).

In addition, approximately 2-5 tests of the epibenthic foraminifera *Cibicides mabahethi* and of the deep infaunal species
160 *Globobulimina affinis* s.l. were selected from the size fraction > 125 μm of core SO-236-052-4. Stable oxygen and carbon isotope analyses were performed with Finnigan MAT 253 gas mass spectrometers coupled to automatic carbonate preparation devices Kiel II or IV, respectively. The mass spectrometers were calibrated to the PDB scale via international standard NBS19, and results are given in δ-notation versus VPDB. Based on measurements of an internal laboratory standard



(Solnhofen limestone) together with samples over a 1-year period, precision was better than 0.08 ‰ for $\delta^{18}\text{O}$ and 0.06 ‰ for $\delta^{13}\text{C}$, respectively.

For site SO-236-052 changes in bottom water oxygen concentrations were estimated based on the $\delta^{13}\text{C}$ difference between the epifaunal (*C. mabahethi*) and deep infaunal (*G. affinis* s.l.) benthic foraminifera using the function $\Delta\delta^{13}\text{C} = 0.00772 \times [\text{O}_2] + 0.41446$, wherein concentrations $[\text{O}_2] < 235 \mu\text{mol kg}^{-1}$ are considered as significant (Hoogakker et al., 2015). For comparison, oxygen concentration changes of a deep sea sediment core from an Arabian Sea site (GeoB3004, 1803 m water depth) were taken from Schmiedl and Mackensen (2006). These data based on the difference between the epifaunal *Cibicides wuellerstorfi* and *G. affinis*. Further, the $\delta^{13}\text{C}$ gradient between *G. ruber* (white) and *C. mabahethi* of core SO-236-052-4 was estimated for assess the sea surface and bottom-water stable carbon isotope difference and water column mixing.

2.5 Radiocarbon dating and compilation of the age model

Accelerator Mass Spectrometry (AMS) radiocarbon dating was carried out at the Beta Analytic Radiocarbon Dating Laboratory on mixed surface-dwelling planktonic foraminifera from 35 cm, 80 cm and 140 cm depth of core SO-236-052-4 (Table 1). Conventional radiocarbon ages were calibrated using the radiocarbon calibration program CALIB (version 7.0.4; Stuiver and Reimer, 1993) and the calibration curve Marine13 (Reimer et al., 2013). Local reservoir corrections were not applied. Additional age tie points were derived from graphical correlation of the benthic $\delta^{18}\text{O}$ record of core SO-236-052-4 with the LR04 standard benthic stack (Lisiecki and Raymo, 2005) using the software AnalySeries 2.0 (version 5/2005; Paillard et al., 1996). The age model of core M74/4-1143 (Betzler et al., 2013b) was revised by graphical correlation with the planktonic $\delta^{18}\text{O}$ record of core SO-236-052-4 (Fig. 2).

3 Results

3.1 Age model and sedimentation rate

Based on the radiocarbon ages and the alignment of the stable oxygen isotope stratigraphy, core SO-236-052-4 comprises sediments of the past 207.7 ka, respectively (Fig. 2). The top 6 m of sediment core M74/4-1143 comprise the past 242.3 ka. Average sedimentation rates varied between 3.5 cm ka^{-1} in SO-236-052-4 and 4.4 cm ka^{-1} in M74/4-1143. Maximum sedimentation rates occurred during interglacial intervals, with 6.8 cm ka^{-1} (SO-236-052-4) and 8.4 cm ka^{-1} (M74/4-1143) for the Eemian, and 7.1 cm ka^{-1} (SO-236-052-4) to 3.0 cm ka^{-1} (M74/4-1143) for the Holocene (Fig. 2).

3.2 Foraminiferal stable oxygen and carbon isotope records

The $\delta^{18}\text{O}$ values of core SO-236-052-4 vary between -3.09 and -0.68 ‰ in the planktonic *G. ruber*, between 0.91 and 2.51 ‰ in the epibenthic *C. mabahethi*, and between 1.10 and 5.02 ‰ in the deep infaunal *G. affinis* (Fig. 3). Generally, the $\delta^{18}\text{O}$



records reveal a consistent picture with relatively higher values during glacial intervals and lower values during interglacial intervals.

The $\delta^{13}\text{C}$ values of core SO-236-052 vary between 0.12 and 1.25 ‰ in *G. ruber*, between 0.22 and 0.91 ‰ in *C. mabahethi*, and between -0.84 to 0.27 ‰ in *G. affinis* (Fig. 3). Despite considerable short-term variability, all records reveal a stepwise increase of $\delta^{13}\text{C}$ values with lowest values during the Marine Isotope Stage (MIS) 6 and highest values during the Holocene (Fig. 3).

Considering the past bottom-water oxygen concentration reconstruction for core SO-236-052-4 by using the $\Delta\delta^{13}\text{C}_{\text{Cm-Ga}}$ estimation, the values varied between 10.43 and 139.45 $\mu\text{mol kg}^{-1}$ with average values of approximately 65.50 $\mu\text{mol kg}^{-1}$. In addition, a long-lasting oxygen depletion was observed, starting from the end of MIS 5 to the end of MIS 3 (duration of ~50 ka), and with average oxygen concentrations of approximately 52.50 $\mu\text{mol kg}^{-1}$. The oxygen concentration of sediment core GeoB3004 (W Arabian Sea) showed an average oxygen content of approximately 81.75 $\mu\text{mol kg}^{-1}$ (Schmiedl and Mackensen, 2006). In comparison both cores represented a precessional pattern during MIS 6 to late MIS 5, in which they were almost in phase. A comparable long lasting oxygen depletion, as documented at site SO-236-052, could not be identified for GeoB3004.

The $\Delta\delta^{13}\text{C}_{\text{Cm-Ga}}$ calculation for site SO-236-052 showed maximum differences of the planktic and epibenthic stable $\delta^{13}\text{C}$ values during the full interglacial periods of MIS 7, 5 and 1, coinciding with the global sea-level highstands. Accordingly, minimum differences were documented for the glacial periods MIS 6 and 2 and sea-level lowstands.

3.3 Sedimentological and geochemical records

The detailed sedimentological and geochemical data of core SO-236-052-4 reveal a glacial-interglacial pattern but also considerable short-term variability (Figs. 4a-d). Sortable silt records are available for both sites and in general they show coarser means in interglacial times (Figs. 4a, 5). However, absolute values and variability are much greater in core M74/4-1143 which is located in the drift of the Kardiva Channel (Betzler et al., 2013b) compared to core SO-236-052-2 from the more sheltered southern part of the Inner Sea. In core M74/4-1143, sortable silt shows an increase towards the MIS 6/5 transition (Termination II) followed by generally elevated values during the MIS 5.5, whereas there is much less variability at the same time in the data from core SO-236-052-4. Both cores show a coarsening of the sortable silt towards the MIS 1.

Bulk mean grain size shows a pronounced glacial-interglacial variability with up to 57 μm during the MIS 2 and MIS 6 and values between 10 and 30 μm for the remainder (Fig. 4a). Finest sediments occur during the early MIS 5 and the MIS 1.

Total Organic Carbon (TOC) and carbonate (CaCO_3) content of core SO-236-052-4 reveal reverse glacial-interglacial trends with maximum TOC content during glacial- and maximum carbonate contents during interglacial periods. TOC varies between 0.85 wt. % (interglacial) and 2.06 wt. % (glacial), whereas the carbonate content varies between 77.03 wt. % (glacial) and 89.40 wt. % (interglacial) (Fig. 4b).



The Fe/Ca and Si/Ca records reveal generally higher values during glacial and lower values during interglacial periods. Both Fe/Ca and Si/Ca records are characterized by an abrupt and short-lasting maximum at Termination II (Fig. 4c). The Ba/Ca ratio is comparatively low but shows a similar glacial-interglacial pattern, such as the Fe/Ca and Si/Ca records, with generally higher ratios during glacial periods and lower ratios during interglacial periods, but with additional variability on orbital time scales (Fig. 4d). Inverse patterns are observed for the Sr/Ca record, which follows the inversed $\delta^{18}\text{O}$ curve and shows higher values during interglacial and lower values during glacial periods (Fig. 4d).

3.4 Benthic foraminiferal record

In sediment core SO-236-052-4, a total of 256 different benthic foraminiferal species were distinguished, with 51 to 93 different species per sample. The diversity $H(S)$ of core SO-236-052-4 is relatively high and varies between 3.3 and 4.0, with a slight long-term decrease towards today (Fig. 6a). The three-component model of the Q-mode PCA explains 89.14 % of the total variance (Fig. 6, Table 2). Assemblage 1 (PC1) explains 31.54 % of the total variance and is dominated by *N. proboscidea* and *D. araucana*, with *Hyalinea inflata*, *Cymbaloporeta squamosa*, *Bulimina marginata* and *Rosalina vilardeboana* as associated taxa. This assemblage occurred mainly during the late MIS 7 and 5 and is less pronounced during MIS 4 to early MIS 2 (Fig. 6b). Assemblage 2 (PC2) explains 30.54 % of the total variance and is dominated by *C. mabahethi*, with *Discorbinella bertheloti*, *Siphogenerina columellaris*, *Gyroidina umbonata*, *Reophax* sp., *H. inflata*, and *D. araucana* as associated taxa (Table 2). The assemblage 2 occurred mainly during MIS 6 and 1 (Fig. 6c). Assemblage 3 (PC3) explains 27.06 % of the total variance and is dominated by *N. proboscidea* and *Hoeglundina elegans*, with *D. bertheloti*, *Cibicidoides subhaidingeri*, *Discorbis* sp., *Spiroplectinella sagittula* s.l., and *C. mabahethi* as associated taxa (Table 2). Assemblage 3 occurred during MIS 4 to 2 (Fig. 6d).

The distribution of the most important benthic foraminiferal species, which characterize the three faunal assemblages, are displayed in Figs. 6e-g. The most abundant species include *C. mabahethi* (maximum relative abundance of ~17 % during MIS 6), the weakly hispid *N. proboscidea* (maximum of ~16 % at the end of MIS 5) and *D. araucana* (maximum of ~11 % during the onset of MIS 5). Meroplanktonic benthic foraminifera (genera *Cymbaloporeta* and *Tretomphaloides*) occurred in elevated numbers during interglacial periods, particularly during MIS 5 (Figs. 5d and 6e).

The foraminiferal fauna at the Inner Sea is dominated by hyaline taxa. In comparison, agglutinated individuals were less abundant, but with increasing relative abundances up to approximately ≥ 20 % of the entire fauna during the glacial periods.

4 Discussion

4.1 Monsoon variability, dust fluxes and marine productivity

The Fe/Ca and Si/Ca ratios at site SO-236-052 were interpreted as proxies for terrigenous sediment delivery, deposited by aeolian dust fluxes in the Maldives Inner Sea. Local sources of Fe-rich sediments can be excluded since the sediments of the Maldives islands and adjacent deep-water environments are characterized by carbonates comprising reef and lagoon



carbonates of the islands and pelagic deep-water carbonates (Betzler et al., 2013b; Reolid et al., 2017). Calcite content is also very high at site SO-236-052 throughout the past 200 ka (Fig. 4b). Studies on modern aerosols of the North Pacific region indicate that most of the oceanic iron input is derived from atmospheric transport after mobilisation from the central Asian deserts and Chinese loess plateau (Duce and Tindale, 1991). Accordingly, the most likely dust sources for the observed Fe in
265 the sediments of the Maldives are the Indian subcontinent and the Asian desert and loess areas (Roberts et al., 2011), although a minor contribution from Africa and Arabia cannot be excluded (Sirocko and Lange, 1991; Chauhan and Shukla, 2016). Coincident to the prevailing wind system, the majority of dust is transported via the NE monsoon, which blows during northern hemisphere winter. Elevated Fe/Ca ratios during the glacial intervals of MIS 6 and MIS 4-2 indicate the combined effects of enhanced glacial dust availability in the source areas and dust transport to the Maldives with generally
270 strengthened NE monsoon winds. Enhanced glacial dust fluxes were also observed in the Arabian Sea associated with a strengthening of northwesterly winds, which blow dust from the Arabian peninsula into the marine areas (deMenocal et al., 1991; Sirocko and Lange, 1991). On a global scale, the generally colder and drier glacial conditions resulted in a two- to fivefold increase of dust fluxes (Maher et al., 2010). Enhanced glacial dust concentrations were also detected in polar ice cores (Ruth et al., 2003; EPICA Community Members, 2004) and a multitude of marine records (deMenocal et al., 1993; Liu
275 et al., 1999; Zhang et al., 1999; Winckler et al., 2008; Maher et al., 2010).

The observed response of the winter circulation of the Maldives to glacial conditions is in line with the finding of a general strengthening of the NE Indian monsoon after initiation of the northern hemisphere glaciation (Gupta and Thomas, 2003). However, our Fe/Ca record lacks significant variability on the precessional band, which should be expected if the dust fluxes were directly proportional to the intensity of the winter monsoon (Caley et al., 2011a, b). Therefore the dust record of
280 the Maldives Inner Sea is mainly driven by the generally enhanced dust availability during glacial intervals. As a major dust source, the Chinese loess plateau is strongly influenced by the East Asian Monsoon (EAM). During the late Quaternary, EAM and related vegetation changes are characterized by predominant excentricity cycles associated with the advance and retreat of the boreal ice sheets (Ding et al., 1995; Liu et al., 1999; Sun et al., 2006; Hao et al., 2012). On the Chinese loess plateau the onset of glacial conditions led to an abrupt increase of atmospheric dust loadings (Zhang et al., 2002) suggesting
285 the operation of climate-vegetation feedbacks. Enhanced deposition of dust particles at site SO-236-052 led to a generally coarsening of the glacial sediment (Fig. 4a) and fostered the distribution of agglutinated benthic foraminifera, which reach a relative abundance of up to ~20 % during the last glacial period (Fig. 7e). Most agglutinated foraminifera in core SO-236-052-4 belong to the Textulariida, such as *Spiroplectammina sagittula*, *Textularia calva* or *Textularia pala*. These and related taxa are often associated with relatively coarse-grained substrates and preferentially use siliciclastic grains for test
290 construction (Allen et al., 1999; Murray, 2006; Armynot du Châtelet et al., 2013).

The equatorial Indian Ocean is limited in the micronutrient iron (Wiggert et al., 2006; Maher et al., 2010) and therefore, enhanced Fe fluxes during glacial periods may have resulted in increased surface water productivity, similar to observations from the Southern Ocean (Anderson et al., 2014; Martínez-García et al., 2014) and the equatorial Pacific Ocean (Costa et al.,



295 2016). The TOC and Ba contents of marine sediments are widely used as proxies for organic matter fluxes and surface water productivity (Müller and Suess, 1979; Gingele et al., 1999; McManus et al., 1999; Rühlemann et al., 1999). But the applicability of both proxies in quantitative reconstructions is limited by the specific sedimentological and biogeochemical processes at the sediment-water interface, including the bulk accumulation rate and bottom water oxygenation (Möbius et al., 2011; Schoepfer et al., 2015; Naik et al., 2017).

Elevated TOC and Ba/Ca values in core SO-236-052-4 suggest generally enhanced organic matter fluxes during glacial 300 periods, which may reflect the influence of Fe fertilisation (Fig. 7b-d). The benthic foraminiferal faunas at site SO-236-052 reveal a marked glacial-interglacial pattern (Figs. 6, 7f). The diversity, microhabitat partitioning and species composition of deep-sea benthic foraminiferal faunas is mainly controlled by the combined influences of quantity and quality of food supply and oxygen content of the bottom and pore waters (Jorissen et al., 1995; Fontanier et al., 2002). The diversity of the faunas is high, with H(S) values always > 3.2, throughout the studied time interval, suggesting the absence of extreme environmental 305 conditions at the sea floor of the study site. Therefore, the observed faunal changes likely reflect variations in the amount and quality of food supply.

The most abundant species of the three benthic foraminiferal assemblages comprise *C. mabahethi*, *N. proboscidea* and *D. araucana*, all with PC scores > 3 in at least one assemblage (Table 2). Microhabitat studies demonstrated that most species of the genera *Cibicides* and *Cicidoides* live as suspension feeders on or elevated above the sea floor (Lutze and Thiel, 310 1989; Linke and Lutze, 1993), therefore we assume a similar microhabitat preference for *C. mabahethi*. In the Red Sea this species is adapted to relatively high oxygen contents and low organic matter fluxes (Edelman-Furstenberg et al., 2001; Badawi et al., 2005). The cosmopolitan *N. proboscidea* inhabits an epifaunal to very shallow infaunal microhabitat (Fontanier et al., 2002; Licari et al., 2003) and has been described as detritus feeder from various bathyal and abyssal environments. In the South Atlantic Ocean, *N. proboscidea* is associated with well-ventilated and oligotrophic conditions 315 (Schmiedl et al., 1997). Whereas this species thrives under moderate to high organic matter fluxes and oxygen-depleted intermediate waters in the Indian Ocean (Murgese and De Deckker, 2007; De and Gupta, 2010) and was used as a proxy for the strength of the SW monsoon (Gupta and Srinivasan, 1992; Gupta and Thomas, 2003; Sarkar and Gupta, 2014). These observations and the high relative abundance of *N. proboscidea* in core SO-236-052-4 during the last glacial intervals MIS 4-2, as well as the interglacial interval MIS 5 suggest an adaptation to a wide range of trophic conditions and confirms its 320 tolerance to moderate oxygen depletion. Little information is available on the ecology of *D. araucana* but its flat trochospiral morphology and distribution in the North Atlantic Ocean suggest an epifaunal microhabitat and adaptation to suspended food sources (Corliss and Chen, 1988; Koho et al., 2008). Similar to the closely related *D. bertheloti* it may prefer mesotrophic and oxic conditions (De, 2010) with a tolerance to moderate oxygen depletion (Edelmann-Furstenberg et al., 2001). The shallow infaunal *Hoeglundina elegans* is commonly associated with low to moderate organic matter fluxes, fresh 325 phytodetritus and high oxygen contents (Corliss, 1985; Koho et al., 2008).



The ecological preferences of the dominant taxa suggest that faunal changes at site SO-236-052, although pronounced, were driven by rather subtle changes in the amount of organic matter fluxes. Instead, the faunal changes likely reflect variations in lateral suspension of food particles, substrate-specific development of infaunal niches, and the influence of oxygen changes on the quality of the organic matter. The high dominance of the detritus feeders *N. proboscidea* and *H. elegans* in assemblage 3 suggest highest organic matter fluxes during the last glacial MIS 4-2 (Fig. 7f). In contrast, the dominance of the epifaunal suspension feeder *C. mabahethi* in assemblage 2 during the penultimate glacial (MIS 6) suggests relatively lower organic matter fluxes. The *N. proboscidea*/*D. araucana* assemblage 1 of MIS 5 reveals some similarity to assemblage 3 but the high abundance of *D. araucana* suggests an overall lower food flux with a considerable amount of suspended particles. In addition, the relatively finer-grained substrate likely opened infaunal niches as indicated by the presence of the shallow to deep infaunal *Bulimina marginata* during the MIS 5 (Jorissen and Wittling, 1999) (Fig. 6e).

While the benthic foraminiferal fauna preliminary show changes on glacial-interglacial time scale, the TOC content and Ba/Ca ratio are characterized by additional variability in the precessional band. The surface water productivity of the northern Indian Ocean is strongly linked to wind-induced mixing of the upper water column and upwelling of nutrient-rich subsurface waters and thus reveals a close association with seasonal changes of the monsoonal wind system (Nair et al., 1989). Accordingly, productivity changes in the northern and northwestern Arabian Sea are coherent to the strength of the SW monsoon (Ivanova et al., 2003; Leuschner and Sirocko, 2003; Singh et al., 2011), and along the Indian west coast to the strength of the NE monsoon (Rostek et al., 1997; Singh et al., 2011). Elevated TOC and Ba/Ca ratios at site SO-236-052 during phases of reduced northern hemisphere summer insolation suggest a direct influence of the Indian winter monsoon on productivity and related organic matter fluxes of the Maldives Inner Sea during the past 200 ka, which is consistent with the present-day situation (de Vos et al. 2014). The close link between the winter monsoon intensity and surface water productivity in the study area is confirmed by the difference between the $\delta^{13}\text{C}$ values of the epipelagic *G. ruber* (Gr) and the epibenthic *C. mabahethi* (Cm) (Figs. 3, 8). Low $\Delta\delta^{13}\text{C}_{\text{Gr-Cm}}$ values indicate enhanced vertical mixing of the water column, which is associated with increased supply of nutrients from subsurface waters into the photic zone, based on enhanced surface water productivity.

350

4.2 Sea-level changes, sedimentation processes and benthic ecosystem dynamics

The close association of changes in sediment composition (i.e. bulk grain size, carbonate content) at site SO-236-052 with the LR04 stable benthic isotope stack (Lisiecki and Raymo, 2005) suggest a dominant influence of sea-level changes on the depositional environments of the Maldives Inner Sea. This is also corroborated by the Sr/Ca variations in the core. In periplatform ooze, i.e. areas around shallow water carbonate banks, higher Sr contents are a consequence of higher input of shallow water aragonite (Dunbar and Dickens, 2003), which is produced in the neritic parts of the platforms and exported to the areas around the platform by currents.

355



The observed changes in bottom currents likely influenced the lateral transport of suspended organic particles as is suggested by variations in the relative abundance of suspension feeders in the different benthic foraminiferal assemblages (Figs. 6, 7, Table 2). The dominance of *D. araucana* during MIS 5 and *C. mabahethi* during MIS 6 and MIS 1 indicate phases of enhanced lateral food supply, which for the interglacial periods (MIS 5, MIS 1) correlate with reconstructed higher current velocities (Fig. 5). The interglacial intervals of SO-236-052-4 (mainly MIS 5 and MIS 7, Fig. 5) contain high abundances of meroplanktonic benthic foraminifera (*Cymbaloporeta*, *Tretomphaloides*), which build floating chambers for dispersal (Banner et al., 1985; Alve, 1999). These taxa are commonly found in shelf environments (Milker and Schmiiedl, 2012). Their acme during the last interglacial maximum at bathyal depth of the Maldives Inner Sea coincides with almost absence of other displaced species from reef and lagoon environments, such as *Elphidium*, *Amphistegina* or *Operculina* (Parker and Gischler, 2011). This implies a repeated colonization of bathyal environments with meroplanktonic taxa from submerged neritic environments during sea-level highstands and strengthened bottom water velocity.

4.3 Changes in intermediate water circulation and oxygenation

The epibenthic stable carbon isotope record of core SO-236-052-4 lacks a coherent glacial-interglacial pattern but reveals an overall $\delta^{13}C_{Cm}$ increase of ~ 0.5 ‰ over the past 200 ka (Fig. 3). Long-term trends of similar magnitude have been recorded from sites bathed by the Antarctic Intermediate Water mass (AAIW) in the southwestern Pacific Ocean (Pahnke and Zahn, 2005; Elmore et al., 2015; Ronge et al., 2015). The general resemblance of the various epibenthic $\delta^{13}C$ records suggests a significant role of AAIW in ventilation of bathyal environments of the Maldives Inner Sea, which is consistent with the modern oceanographic situation (You, 1998).

Following the approach of Hoogakker et al. (2015) we estimated changes in the oxygen content of the intermediate water mass of the Maldives Inner Sea based on the $\Delta\delta^{13}C_{Cm-Ga}$ signal, i.e. the difference between the $\delta^{13}C$ values of the epifaunal *C. mabahethi* and the deep infaunal *G. affinis* s.l. The resulting O_2 concentrations never dropped substantially below $45 \mu\text{mol kg}^{-1}$ ($\sim 1 \text{ ml l}^{-1}$) (Fig. 8). Moreover, the oxic to low oxic conditions ($O_2 > 1 \text{ ml l}^{-1}$) did not seem to pose stress to the benthic foraminiferal fauna. Instead, the proportion of the deep infauna increases exponentially under dysoxic conditions, i.e. at O_2 values significantly below 1 ml l^{-1} (Jorissen et al., 2007). The lack of dysoxic conditions at site SO-236-052 at any time of the past 200 ka is corroborated by the persistent high diversity across glacial and interglacial periods and the low abundance of deep infaunal taxa.

The reconstructed O_2 record reveals precessional changes between oxic and low oxic conditions during northern hemisphere insolation maxima and minima, respectively. Detailed stable isotope records from the southwestern Pacific Ocean indicate enhanced AAIW formation during warm intervals (Pahnke and Zahn, 2005; Elmore et al., 2015; Ronge et al., 2015). Accordingly, the strength of the Oxygen Minimum Zone (OMZ) at the Maldives Inner Sea, which is preconditioned by the southward expansion of the OMZ from the Arabian Sea (Reid, 2003), is controlled by the inflow of the AAIW from the Subantarctic Southern Ocean and thus contains a strong southern hemisphere climate signal. The reconstructed O_2



changes in intermediate waters at site SO-236-052 resemble those from the deep OMZ of the western Arabian Sea, which is influenced by the advection of oxygen-rich North Atlantic Deep Water (NADW) (Schmiedl and Mackensen, 2006). The dependence of oxygen changes in Indian Ocean intermediate and deep-water masses from the inflow of Atlantic and Antarctic water masses is corroborated by a number of recent observations from the northwestern and southeastern Arabian Sea (Pattan and Pearce, 2009; Das et al., 2017; Naik et al., 2017).

The long period of lowered O₂ values below 60 μmol kg⁻¹ centred at MIS 4-3 coincides with a marked monsoon and upwelling maximum in the Arabian Sea (Hermelin and Shimmiedl, 1995; Clemens and Prell, 2003; Leuschner and Sirocco, 2003; Caley et al., 2011a, b), which caused a strengthening and deepening of the OMZ (Almogi-Labin et al., 2000; Den Dulk et al., 2000; Schmiedl and Leuschner, 2005). The expansion of the Arabian Sea OMZ southward into the equatorial region likely preconditioned the oxygen levels of intermediate waters of the Maldives Inner Sea. There, oxygen changes were further lowered by the reduced glacial advection of oxygen-rich AAIW and enhanced regional microbial oxygen consumption reflecting a superposition of high and low-latitude climate signals. The resulting changes in biogeochemical processes at site SO-236-052 are illustrated by the establishment and long-term persistence of the benthic foraminiferal assemblage 3 underlining the positive response of *N. proboscidea* and associated species such as *H. elegans* and *D. bertheloti* to moderately reduced oxygen and increased food levels.

Abrupt O₂ drops occur at the end of the last two glaciations suggesting short phases of reduced AAIW advection or increased surface water productivity and related oxygen consumption at depth (Fig. 8). The recorded events correlate with phases of increased Agulhas leakage, which have been linked to a strengthening of the Indian monsoon and Indian Ocean equatorial winds (Peeters et al., 2004). Accordingly, an additional impact of changes in the strength of the Indian Ocean Equatorial Westerlies (IEW) on environmental changes of the Maldives Inner Sea appears likely (Beaufort et al., 1997, 2001). However, our new results imply that on orbital time scales changes of the winter monsoon and AAIW advection seem to play the dominant role.

5 Conclusions

The integrated evaluation of sedimentological, geochemical and micropaleontological proxy records from the Maldives Inner Sea (tropical Indian Ocean) furthers our understanding of links between equatorial climate variability, sea-level changes, changes in intermediate water ventilation and benthic ecosystem dynamics on orbital time scales during the past 200 ka. The main conclusions are:

(1) Aeolian dust fluxes were considerably enhanced during glacial intervals (MIS 6 and MIS 4-2) as indicated by increased Fe/Ca and Si/Ca ratios, generally coarsening of the bulk sediment, and increased abundance of agglutinated benthic foraminiferal taxa, which use siliciclastic grains for test formation. The enhanced dust input was linked to phases of



generally increased atmospheric dust loads and northeast winds, suggesting a close link of Maldives marine environments to the aridity of the central Asian loess areas and the strength of the Indian winter monsoon.

(2) Increased vertical mixing during glacial phases of intensified winter monsoon resulted in enhanced surface water productivity and associated organic carbon fluxes to the sea-floor as indicated by TOC values and composition of the benthic foraminiferal fauna. The *Cibicidoides mabahethi* (assemblage 2) and *Neouvigerina proboscidea* (assemblage 3) faunas dominate during MIS 6 and MIS 4-2 respectively, suggesting differences in the amount and quality of the food delivery for the two glacial intervals. The $\Delta\delta^{13}C_{Gr-Cm}$, Ba/Ca and TOC records reveal additional changes on the precessional band, which are inversely correlated to northern hemisphere summer insolation underlining a close link of regional vertical mixing of the water column and marine productivity to the Indian winter monsoon.

(3) Glacial-interglacial changes in sea level controlled the downslope transport of sediment from the Maldives islands to the deep-sea environments and influenced the current strength at the benthic boundary layer of the Inner Sea resulting in different grain size and substrates. Hand in hand with sea level changes there was a change in the bottom current regime. The drift deposits recovered by core M74/4-1143 show that highest current intensities occurred during and after the glacial terminations (Fig. 5). Bottom currents in general were stronger during interglacials than during glacials, although core SO-236-052-4 records lower current velocities and lower amplitude of change. Strongest current intensities at the sea floor likely favoured the distribution of certain suspension feeding benthic foraminiferal taxa, such as *D. araucana*.

(4) The long-term trend in the benthic $\delta^{13}C$ record mirrors the basin-wide change in the composition of intermediate waters, implying a close linkage to the main formation sites of the AAIW in the Southern Ocean. The precessional changes of estimated oxygen concentrations of intermediate waters are coherent with changes in the deep Arabian Sea. This suggests an influence of the lateral expansion of oxygen minimum waters from the Arabian Sea into the equatorial intermediate Indian Ocean and modulation by inflowing AAIW from the south. The predominance of *N. proboscidea* during a long phase of reduced oxygen concentrations (with average oxygen concentrations around $50 \mu\text{mol kg}^{-1}$) during late MIS 5 to late MIS 3 suggests an adaption of this species to the particular biogeochemical conditions and food quality associated with low oxie conditions.

Acknowledgements

We thank the masters and crews as well as the shipboard scientific parties of R/V SONNE SO236 and R/V METEOR M74/4 cruises for their excellent collaboration. Jutta Richarz is thanked for her support during grain size analyses, and Lisa Schönborn and Günther Meyer for technical support during stable isotope measurements. This research used data acquired at the XRF Core Scanner Lab at the MARUM, Center for Marine Environmental Sciences, University of Bremen, Germany. This study was supported by grants 03G0236A of the Federal Ministry of Education and Research. The Ministry of Fisheries and Agriculture of the Maldives is thanked for granting the research permit for Maldivian waters.



455 **References**

- Allen, K., Roberts, S., and Murray, J. W.: Marginal marine agglutinated foraminifera: affinities for mineral phases, *Journal of Micropaleontology*, 35, 183–191, doi: 10.1144/jm.18.2.183, 1999.
- Almogi-Labin, A., Schmiedl, G., Hemleben, C., Siman-Tov, R., Segl, M., and Meischner, D.: The influence of the NE winter monsoon on productivity changes in the Gulf of Aden, NW Arabian Sea, during the last 530 ka as recorded by foraminifera, *Marine Micropaleontology*, 40, 295–319, doi: 10.1016/S0377-8398(00)00043-8, 2000.
- 460 Alve, E.: Colonization of new habitats by benthic foraminifera: a review, *Earth-Science Reviews*, 46, 167–185, doi: 10.1016/S0012-8252(99)00016-1, 1999.
- Anderson, R. F., Barker, S., Fleisher, M., Gersonde, R., Goldstein, S. L., Kuhn, G., Mortyn, P. G., Pahnke, K., and Sachs, J. P.: Biological response to millennial variability of dust and nutrient supply in the Subantarctic South Atlantic Ocean, *Philosophical Transactions of the Royal Society A*, 372, 1–17, doi: 10.1098/rsta.2013.0054, 2014.
- 465 Armynot du Châtelet, E., Bout-Roumazeilles, V., Coccioni, R., Frontalini, F., Guillot, F., Kaminski, M. A., Recourt, P., Riboulleau, A., Trentesaux, A., Tribovillard, N., and Ventalon, S.: Environmental control on shell structure and composition of agglutinated foraminifera along a proximal-distal transect in the Marmara Sea, *Marine Geology*, 335, 114–128, doi: 10.1016/j.margeo.2012.10.013, 2013.
- 470 Backhaus, K., Erichson, B., Plinke, W., and Weiber, R.: *Multivariate Analysemethoden*, Springer, Berlin, Heidelberg, New York, 1–575, 2008.
- Badawi, A., Schmiedl, G., and Hemleben, C.: Impact of late Quaternary environmental changes on deep-sea benthic foraminiferal faunas of the Red Sea, *Marine Micropaleontology*, 58, 13–30, doi: 10.1016/j.marmicro.2005.08.002, 2005.
- Banner, F. T., Pereira, C. P. G., and Desai, D.: "Tretomphaloid" float chambers in the Discorbidae and Cymbaloporidae, *Journal of Foraminiferal Research*, 15, 159–174, doi: 10.2113/gsjfr.15.3.159, 1985.
- 475 Beaufort, L., Lancelot, Y., Camberlin, P., Cayre, O., Vincent, E., Bassinot, F., and Labeyrie, L.: Insolation cycles as a major control of equatorial Indian Ocean Primary Production, *Science*, 278, 1451–1454, doi: 10.1126/science.278.5342.1451, 1997.
- Beaufort, L., de Garidel-Thoron, T., Mix, A. C., and Pisias, N. G.: ENSO-like forcing on oceanic primary production during the Late Pleistocene, *Science*, 293, 2440–2444, doi: 10.1126/science.293.5539.2440, 2001.
- 480 Betzler, C., Hübscher, C., Lindhorst, S., Reijmer, J. J. G., Römer, M., Droxler, A. W., Fürstenau, J., Lüdmann, T.: Monsoonal-induced partial carbonate platform drowning (Maldives, Indian Ocean), *Geology*, 37, 867–870, doi: 10.1130/G25702A.1, 2009.
- Betzler, C., Fürstenau, J., Lüdmann, T., Hübscher, C., Lindhorst, S., Paul, A., Reijmer, J. J. G., and Droxler, A. W.: Sea-level and ocean-current control on carbonate-platform growth, Maldives, Indian Ocean, *Basin Research*, 25, 172–196, doi: 10.1111/j.1365-2117.2012.00554.x, 2013a.
- 485



- Betzler, C., Lüdmann, T., Hübscher, C., and Fürstenau, J.: Current and sea-level signals in periplatform ooze (Neogene, Maldives, Indian Ocean), *Sedimentary Geology*, 290, 126–137, doi: 10.1016/j.sedgeo.2013.03.011, 2013b.
- Betzler, C., Eberli, G. P., Kroon, D., Wright, J. D., Swart, P. K., Nath, B. N., Alvarez-Zarikian, C. A., Alonso-García, M.,
490 Bialik, O. M., Blättler, C. L., Guo, J. A., Haffen, S., Horozal, S., Inoue, M., Jovane, L., Lanci, L. Laya, J. C., Mee, A. L.
H., Lüdmann, T., Nakakuni, M., Niino, K., Petruny, L. M., Pratiwi, S. D., Reijmer, J. J. G., Reolid, J., Slagle, A. L.,
Sloss, C. R., Su, X., Yao, Z., and Young, J. R.: The abrupt onset of the modern South Asian Monsoon winds, *Scientific
Reports*, 6, 29838, doi: 10.1038/srep29838, 2016.
- Bianchi, G. G., Hall, I. R., McCave I. N., and Joseph, L.: Measurement of the sortable silt current speed proxy using the
495 Sedigraph 5100 and Coulter Multisizer IIe: Precision and accuracy, *Sedimentology*, 46, 1001–1014, doi: 10.1046/j.1365-
3091.1999.00256.x, 1999.
- Blott, S. J. and Pye, K.: GRADISTAT: a grain size distribution and statistics package for the analysis of unconsolidated
sediments, *Earth Surface Processes and Landforms*, 26, 1237–1248, doi: 10.1002/esp.261, 2001.
- Caley, T., Malaizé, B., Zaragosi, S., Rossignol, L., Bourget, J., Eynaud, F., Martinez, P., Giraudeau, J., Charlier, K., and
500 Ellouz-Zimmermann, N.: New Arabian Sea records help decipher orbital timing of Indo-Asian monsoon, *Earth and
Planetary Science Letters*, 308, 433–444, doi: 10.1016/j.epsl.2011.06.019, 2011a.
- Caley, T., Malaizé, B., Revel, M., Ducassou, E., Wainer, K., Ibrahim, M., Shoeaib, D., Migeon, S., and Marieu, V.: Orbital
timing of the Indian, East Asian and African boreal monsoons and the concept of a ‘global monsoon’, *Quaternary
Science Reviews*, 30, 3705–3715, doi: 10.1016/j.quascirev.2011.09.015, 2011b.
- 505 Chauhan, O. S. and Shukla, A. S.: Evaluation of the influence of monsoon climatology on dispersal and sequestration of
continental flux over the southeastern Arabian Sea, *Marine Geology*, 371, 44–56, doi: 10.1016/j.margeo.2015.10.018,
2016.
- Clemens, S. C. and Prell, W. L.: Late Pleistocene variability of Arabian Sea summer monsoon winds and continental aridity:
Eolian records from the lithogenic component of deep-sea sediments, *Paleoceanography*, 5, 109–145, doi:
510 10.1029/PA005i002p00109, 1990.
- Clemens, S. C. and Prell, W. L.: A 350,000 year summer-monsoon multi-proxy stack from the Owen Ridge, Northern
Arabian Sea, *Marine Geology*, 201, 35–51, doi: 10.1016/S0025-3227(03)00207-X, 2003.
- Clemens, S., Prell, W., Murray, D., Shimmield, G., and Weedon, G.: Forcing mechanisms of the Indian Ocean monsoon,
Nature, 353, 720–725, 1991.
- 515 Corliss, B. H.: Microhabitats of benthic foraminifera within deep-sea sediments, *Nature*, 314, 435–438, doi:
10.1038/314435a0, 1985.
- Corliss, B. H. and Chen, C.: Morphotype patterns of Norwegian Sea deep-sea benthic foraminifera and ecological
implications, *Geology*, 16, 716–719, doi: 10.1130/0091-7613(1988), 1988.



- Costa, K. M., McManus, J. F., Anderson, R. F., Ren, H., Sigman, D. M., Winckler, G., Fleisher, M. Q., Marcantonio, F., and
520 Ravelo, A. C.: No iron fertilization in the equatorial Pacific Ocean during the last ice age, *Nature*, 529, 519–522, doi:
10.1038/nature16453, 2016.
- Croudace, I. W. and Rothwell, R. G.: *Micro-XRF Studies of Sediment Cores: Applications of a non-destructive tool for the
environmental sciences*, Springer, 1-656, 2015.
- Das, M., Singh, R. K., Gupta, A. K., and Bhaumik, A. K.: Holocene strengthening of the oxygen minimum zone in the
525 northwestern Arabian Sea linked to changes in intermediate water circulation or Indian monsoon intensity?
Palaeogeography, Palaeoclimatology, Palaeoecology, doi: 10.1016/j.palaeo.2016.10.035, in press 2017.
- De, S. and Gupta, A. K.: Deep-sea faunal provinces and their inferred environments in the Indian Ocean based on
distribution of Recent benthic foraminifera, *Palaeogeography, Palaeoclimatology, Palaeoecology*, 291, 429–442, doi:
10.1016/j.palaeo.2010.03.012, 2010.
- 530 Debenay, J.-P.: *A Guide to 1,000 Foraminifera from Southwestern Pacific, New Caledonia*, IRD Éditions, Publications
Scientifiques du Muséum, 1–384, 2012.
- deMenocal, P. B., Bloemendal, J., and King, J.: A rock-magnetic record of monsoonal dust deposition to the Arabian Sea:
Evidence for a shift in the mode of deposition at 2.4 Ma, *Proceedings of the Ocean Drilling Program, Scientific Results*,
117, 389–407, 1991.
- 535 deMenocal, P. B., Ruddiman, W. F., and Pokras, E. M.: Influences of high- and low-latitude processes on African terrestrial
climate: Pleistocene eolian records from equatorial Atlantic Ocean Drilling Program Site 663, *Paleoceanography*, 8, 209–
242, doi: 10.1029/93PA02688, 1993.
- Den Dulk, M., Reichert, G. J., van Heyst, S., Zachariasse, W. J., and Van der Zwaan, G. J.: Benthic foraminifera as proxies
of organic matter flux and bottom water oxygenation? A case history from the northern Arabian Sea, *Palaeogeography,*
540 *Palaeoclimatology, Palaeoecology*, 161, 337–359, doi: 10.1016/S0031-0182(00)00074-2, 2000.
- de Vos, A., Pattiaratchi, C. B., and Wijeratne, E. M. S.: Surface circulation and upwelling patterns around Sri Lanka,
Biogeosciences, 11, 5909–5930, doi: 10.5194/bg-11-5909-2014, 2014.
- Ding, Z., Liu, T., Rutter, N. W., Yu, Z., Guo, Z., and Zhu, R.: Ice-Volume Forcing of East Asian Winter Monsoon
Variations in the Past 800,000 Years, *Quaternary Research*, 44, 149–159, doi: 10.1006/qres.1995.1059, 1995.
- 545 Duce, R. A. and Tindale, N. W.: Atmospheric transport of iron and its deposition in the ocean, *Limnology and*
Oceanography, 36, 1715–1726, doi: 10.4319/lo.1991.36.8.1715, 1991.
- Dunbar, G. B. and Dickens, G. R.: Late Quaternary shedding of shallow-water marine carbonate along a tropical mixed
siliciclastic-carbonate shelf: Great Barrier Reef, Australia, *Sedimentology*, 50, 1061–1077, doi: 10.1046/j.1365-
3091.2003.00593.x, 2003.
- 550 Edelman-Furstenberg, Y., Scherbacher, M., Hemleben, C., and Almogi-Labin, A.: Deep-sea benthic foraminifera from the
central Red Sea, *Journal of Foraminiferal Research*, 31, 48–59, 2001.



- Elmore, A. C., McClymont, E. L., Elderfield, H., Kender, S., Cook, M. R., Leng, M. J., Greaves, M., and Misra, S.: Antarctic Intermediate Water properties since 400 ka recorded in infaunal (*Uvigerina peregrina*) and epifaunal (*Planulina wuellerstorfi*) benthic foraminifera, *Earth and Planetary Science Letters*, 428, 193–203, doi: 10.1016/j.epsl.2015.07.013, 555 2015.
- EPICA Community Members: Augustin, L., Barbante, C., Barnes, P. R. F., Barnola, J. M., Bigler, M., Castellano, E., Cattani, O., Chappellaz, J., Dahl-Jensen, D., Delmonte, B., Dreyfus, G., Durand, G., Falourd, S., Fischer, H., Flückiger, J., Hansson, M. E., Huybrechts, P., Jugie, G., Johnsen, S. J., Jouzel, J., Kaufmann, P., Kipfstuhl, J., Lambert, F., Lipenkov, V. Y., Littot, G. C., Longinelli, A., Lorrain, R., Maggi, V., Masson-Delmotte, V., Miller, H., Mulvaney, R., 560 Oerlemans, J., Oerter, H., Orombelli, G., Parrenin, F., Peel, D. A., Petit, J.-R., Raynaud, D., Ritz1, C., Ruth, U., Schwander, J., Siegenthaler, U., Souchez, R., Stauffer, B., Steffensen, J. P., Stenni, B., Stocker, T. F., Tabacco, I. E., Udisti, R., van de Wal, R. S. W., van den Broeke, M., Weiss, J., Wilhelms, F., Winther, J.-G., Wolff, E. W., and Zucchelli, M.: Eight glacial cycles from an Antarctic ice core, *Nature*, 429, 623–628, doi: 10.1038/nature02599, 2004.
- Folk, R. L. and Ward, W. C.: Brazos River Bar: A Study in the Significance of Grain Size Parameters, *Journal of* 565 *Sedimentary Petrology*, 27, 3–26, 1957.
- Fontanier, C., Jorissen, F. J., Licari, L., Alexandre, A., Anschutz, P., and Carbonel, P.: Live benthic foraminiferal faunas from the Bay of Biscay: faunal density, composition, and microhabitats, *Deep-Sea Research I*, 49, 751–785, doi: 10.1016/S0967-0637(01)00078-4, 2002.
- Gingele, F. X., Zabel, M., Kasten, S., Bonn, W. J., and Nürnberg, C. C.: Biogenic barium as a proxy for paleoproductivity: 570 Methods and limitations of application. In: Fischer, G and Wefer, G. (Eds.), *Use of proxies in paleoceanography: Examples from the South Atlantic*, Springer, Berlin, Heidelberg, 345–364, 1999.
- Gupta, A. K. and Srinivasan, M. S.: *Uvigerina proboscidea* abundances and paleoceanography of the northern Indian Ocean DSDP Site 214 during the Late Neogene, *Marine Micropaleontology*, 19, 355–367, doi: 10.1016/0377-8398(92)90038-L, 1992.
- 575 Gupta, A. K. and Thomas, E.: Initiation of Northern Hemisphere glaciation and strengthening of the northeast Indian monsoon: Ocean Drilling Program Site 758, eastern equatorial Indian Ocean, *Geology*, 31, 47–50, doi: 10.1130/0091-7613(2003), 2003.
- Gupta, A. K., Anderson, D. M., and Overpeck, J. T.: Abrupt changes in the Asian southwest monsoon during the Holocene and their links to the North Atlantic Ocean, *Nature*, 421, 354–357, doi: 10.1038/nature01340, 2003.
- 580 Hall, I. R., McCave, I. N., Chapman, M. R., and Shackleton, N. J.: Coherent deep flow variation in the Iceland and American basins during the last interglacial, *Earth and Planetary Science Letters*, 164, 15–21, doi: 10.1016/S0012-821X(98)00209-X, 1998.



- Hao, Q., Wang, L., Oldfield, F., Peng, S., Qin, L., Song, Y., Xu, B., Qiao, Y., Bloemendal, J., and Guo, Z.: Delayed build-up of Arctic ice sheets during 400,000-year minima in insolation variability, *Nature*, 490, 393–396, doi: 10.1038/nature11493, 2012.
- 585
- Hastenrath, S., Nicklis, A., and Greischar, L.: Atmospheric-hydrospheric mechanisms of climate anomalies in the western equatorial Indian Ocean, *Journal of Geophysical Research*, 98, 20219–20235, doi: 10.1029/93JC02330, 1993.
- Hermelin, J. O. R. and Shimmield, G. B.: Impact of productivity events on the benthic foraminiferal fauna in the Arabian Sea over the last 150,000 years, *Paleoceanography*, 10, 85–116, doi: 10.1029/94PA02514, 1995.
- 590
- Holbourn, A., Henderson, A. S., and MacLeod, N.: *Atlas of Benthic Foraminifera*, Wiley-Blackwell, Natural History Museum, 1–642, 2013.
- Hoogakker, B. A. A., Elderfield, H., Schmiedl, G., McCave, I. N., and Rickaby, R. E. M.: Glacial-interglacial changes in bottom-water oxygen content on the Portuguese margin, *Nature Geoscience*, 8, 40–43, doi: 10.1038/ngeo2317, 2015.
- Hottinger, L., Halicz, E., and Reiss, Z.: Recent Foraminifera from the Gulf of Aqaba, Red Sea, Ljubljana, Slovenska Akademija Znanosti in Umetnosti, 1–179, 1993.
- 595
- Ivanova, E., Schiebel, R., Singh, A. D., Schmiedl, G., Niebler, H.-S., and Hemleben, C.: Primary production in the Arabian Sea during the last 135000 years, *Palaeogeography, Palaeoclimatology, Palaeoecology*, 197, 61–82, doi: 10.1016/S0031-0182(03)00386-9, 2003.
- Jones, R. W.: *The Challenger Foraminifera*, The Natural History Museum, London, Oxford University Press, 1–290, 1994.
- 600
- Jorissen, F. J. and Wittling, I.: Ecological evidence from live-dead comparisons of benthic foraminiferal faunas off Cape Blanc (Northwest Africa), *Palaeogeography, Palaeoclimatology, Palaeoecology*, 149, 151–170, doi: 10.1016/S0031-0182(98)00198-9, 1999.
- Jorissen, F. J., de Stigter, H. C., and Widmark, J. G. V.: A conceptual model explaining benthic foraminiferal microhabitats, *Marine Micropaleontology*, 26, 3–15, doi: 10.1016/0377-8398(95)00047-X, 1995.
- 605
- Jorissen, F.J., Fontanier, C. and Thomas, E.: Paleoclimatological proxies based on deep-sea benthic foraminiferal assemblage characteristics. In: Hillaire-Marcel, C. and De Vernal, A. (Eds.), *Proxies in Late Cenozoic paleoceanography*, *Developments in Marine Geology*, Elsevier, Amsterdam, 277–328, 2007.
- Jung, S. J. A., Ganssen, G. M., and Davies, G. R.: Multidecadal variations in the early Holocene outflow of Red Sea Water into the Arabian Sea, *Paleoceanography*, 16, 658–668, doi: 10.1029/2000PA000592, 2001.
- 610
- Koho, K. A., García, R., de Stigter, H. C., Epping, E., Koning, E., Kouwenhoven, T. J., and Van der Zwaan, G. J.: Sedimentary labile organic carbon and pore water redox control on species distribution of benthic foraminifera: A case study from Lisbon–Setúbal Canyon (southern Portugal), *Progress in Oceanography*, 79, 55–82, doi: 10.1016/j.pocean.2008.07.004, 2008.
- Laskar, J., Robutel, P., Joutel, F., Gastineau, M., Correia, A. C. M., and Levrard, B.: A long term numerical solution for the insolation quantities of the Earth, *Astronomy & Astrophysics*, 428, 261–285, doi: 10.1051/0004-6361:20041335, 2004.
- 615



- Leuschner, D. C. and Sirocko, F.: Orbital insolation forcing of the Indian Monsoon - a motor for global climate changes? *Palaeogeography, Palaeoclimatology, Palaeoecology*, 197, 83–95, doi: 10.1016/S0031-0182(03)00387-0, 2003.
- Licari, L. N., Schumacher, S., Wenzhöfer, F., Zabel, M., and Mackensen, A.: Communities and microhabitats of living benthic foraminifera from the tropical East Atlantic: Impact of different productivity regimes, *Journal of Foraminiferal Research*, 33, 10–31, doi: 10.2113/0330010, 2003.
- 620 Linke, P. and Lutze, G. F.: Microhabitat preferences of benthic foraminifera—a static concept or a dynamic adaptation to optimize food acquisition? *Marine Micropaleontology*, 20, 215–234, doi: 10.1016/0377-8398(93)90034-U, 1993.
- Lisiecki, L. E. and Raymo, M. E.: A Pliocene-Pleistocene stack of 57 globally distributed benthic $\delta^{18}\text{O}$ records, *Paleoceanography*, 20, PA1003, 1–17, doi:10.1029/2004PA001071, 2005.
- 625 Liu, T., Ding, Z., and Rutter, N.: Comparison of Milankovitch periods between continental loess and deep sea records over the last 2.5 Ma, *Quaternary Science Reviews*, 18, 1205–1212, doi: 10.1016/S0277-3791(98)00110-3, 1999.
- Loeblich, A. R. and Tappan, H.: *Foraminiferal Genera and their Classification*, Van Nostrand Reinhold Company, New York, 1–2115, 1988.
- Lüdmann, T., Kalvelage, C., Betzler, C., Fürstenauf, J., and Hübscher, C.: The Maldives, a giant isolated carbonate platform dominated by bottom currents, *Marine and Petroleum Geology*, 43, 326–340, doi: 10.1016/j.marpetgeo.2013.01.004, 2013.
- 630 Lutze, G. F. and Thiel, H.: Epibenthic foraminifera from elevated microhabitats: *Cibicoides wuellerstorfi* and *Planulina ariminensis*, *Journal of Foraminiferal Research*, 19, 153–158, doi: 10.2113/gsjfr.19.2.153, 1989.
- Maher, B. A., Prospero, J. M., Mackie, D., Gaiero, D., Hesse, P. P., and Balkanski, Y.: Global connections between aeolian dust, climate and ocean biogeochemistry at the present day and at the last glacial maximum, *Earth-Science Reviews*, 99, 61–97, doi: 10.1016/j.earscirev.2009.12.001, 2010.
- 635 Manighetti, B. and McCave, I. N.: Late glacial and Holocene palaeocurrents through South Rockall Gap, NE Atlantic Ocean, *Paleoceanography*, 10, 611–626, 1995.
- Martínez-García, A., Sigman, D. M., Ren, H., Anderson, R. F., Straub, M., Hodell, D. A., Jaccard, S. L., Eglinton, T. I., and Haug, G. H.: Iron fertilization of the Subantarctic Ocean during the Last Ice Age, *Science*, 343, 1347–1350, doi: 10.1126/science.1246848, 2014.
- 640 McCave, I. N. and Hall, I. R.: Size sorting in marine muds: Processes, pitfalls, and prospects for paleoflow-speed proxies, *Geochemistry, Geophysics, Geosystems*, 7, 1–37, doi: 10.1029/2006GC001284, 2006.
- 645 McCave, I. N., Manighetti, B., and Beveridge, N. A. S.: Circulation in the glacial North Atlantic inferred from grain-size measurements, *Nature*, 374, 149–152, doi: 10.1038/374149a0, 1995a.
- McCave, I. N., Manighetti, B., and Robinson, S. G.: Sortable silt and fine sediment size/composition slicing: Parameters for palaeocurrent speed and palaeoceanography, *Paleoceanography*, 10, 593–610, doi: 10.1029/94PA03039, 1995b.



- McManus, J., Berelson, W. M., Hammond, D. E., and Klinkhammer, G. P.: Barium cycling in the North Pacific:
650 Implications for the utility of Ba as a paleoproductivity and paleoalkalinity proxy, *Paleoceanography*, 14, 53–61, 1999.
- Milker, Y. and Schmiedel, G.: A taxonomic guide to modern benthic shelf foraminifera of the western Mediterranean Sea,
Palaeontologia Electronica, 15, 16A, 1–134, 2012.
- Möbius, J., Gaye, B., Lahajnar, N., Bahlmann, E., and Emeis, K.-C.: Influence of diagenesis on sedimentary $\delta^{15}\text{N}$ in the
Arabian Sea over the last 130 ka, *Marine Geology*, 284, 127–138, doi: 10.1016/j.margeo.2011.03.013, 2011.
- 655 Müller, P. J. and Suess, E.: Productivity, sedimentation rate, and sedimentary organic matter in the oceans - I. Organic
carbon preservation, *Deep-Sea Research*, 26, 1347–1362, doi: 10.1016/0198-0149(79)90003-7, 1979.
- Murgese, D. S. and De Deckker, P.: The Late Quaternary evolution of water masses in the eastern Indian Ocean between
Australia and Indonesia, based on benthic foraminifera faunal and carbon isotopes analyses, *Palaeogeography*,
Palaeoclimatology, *Palaeoecology*, 247, 382–401, doi: 10.1016/j.palaeo.2006.11.002, 2007.
- 660 Murray, J. W.: *Ecology and Applications of Benthic Foraminifera*, Cambridge University Press, 1–426, 2006.
- Naik, D. K., Saraswat, R., Lea, D. W., Kurtarkar, S. R., and Mackensen, A.: Last glacial-interglacial productivity and
associated changes in the eastern Arabian Sea, *Palaeogeography*, *Palaeoclimatology*, *Palaeoecology*, doi:
10.1016/j.palaeo.2016.07.014, in press 2017.
- Nair, R. R., Ittekkot, V., Manganini, S. J., Ramaswamy, V., Haake, B., Degens, E. T., Desai, B. N., and Honjo, S.: Increased
665 particle flux to the deep ocean related to monsoons, *Nature*, 338, 749–751, doi: 10.1038/338749a0, 1989.
- NASA Goddard Space Flight Center, Ocean Ecology Laboratory, Ocean Biology Processing Group: MODIS-Aqua Ocean
Color Data, doi: 10.5067/AQUA/MODIS_OC.2014.0., 2014.
- Olson, D. B., Hitchcock, G. L., Fine, R. A., and Warren, B. A.: Maintenance of the low-oxygen layer in the central Arabian
Sea, *Deep-Sea Research II*, 40, 673–685, doi: 10.1016/0967-0645(93)90051-N, 1993.
- 670 Pahnke, K. and Zahn, R.: Southern hemisphere water mass conversion with North Atlantic climate variability, *Science*, 307,
1741–1746, doi: 10.1126/science.1102163, 2005.
- Paillard, D., Labeyrie, L., and Yiou, P.: Macintosh Program Performs Time-Series Analysis, *Eos Transactions AGU*, 77,
379–379, doi:10.1029/96EO00259, 1996.
- Parker, J. H. and Gischler, E.: Modern foraminiferal distribution and diversity in two atolls from the Maldives, Indian Ocean,
675 *Marine Micropaleontology*, 78, 30–49, doi:10.1016/j.marmicro.2010.09.007, 2011.
- Pattan, J. N. and Pearce, N. J. G.: Bottom water oxygenation history in southeastern Arabian Sea during the past 140 ka:
Results from redox-sensitive elements, *Palaeogeography*, *Palaeoclimatology*, *Palaeoecology*, 280, 396–405, doi:
10.1016/j.palaeo.2009.06.027, 2009.
- Peeters, F. J. C., Acheson, R., Brummer, G.-J. A., de Ruijter, W. P. M., Schneider, R. R., Ganssen, G. M., Ufkes, E., and
680 Kroon, D.: Vigorous exchange between the Indian and Atlantic oceans at the end of the past five glacial periods, *Nature*,
430, 661–665, doi: 10.1038/nature02785, 2004.



- Prasad, T. G. and Ikeda, M.: Seasonal spreading of the Persian Gulf Water mass in the Arabian Sea, *Journal of Geophysical Research*, 106, 17.059–17.071, doi: 10.1029/2000JC000480, 2001.
- Reichert, G. J., Lourens, L. J., and Zachariasse, W. J.: Temporal variability in the northern Arabian Sea Oxygen Minimum
685 Zone (OMZ) during the last 225,000 years, *Paleoceanography*, 13, 607–621, doi: 10.1029/98PA02203, 1998.
- Reid, J. L.: On the total geostrophic circulation of the Indian Ocean: flow patterns, tracers, and transports, *Progress in Oceanography*, 56, 137–186, doi: 10.1016/S0079-6611(02)00141-6, 2003.
- Reimer, P. J., Bard, E., Bayliss, A., Beck, J. W., Blackwell, P. G., Ramsey, C. B., Buck, C. E., Cheng, H., Edwards, R. L.,
Friedrich, M., Grootes, P. M., Guilderson, T. P., Hafliadason, H., Hajdas, I., Hatté, C., Heaton, T. J., Hoffmann, D. L.,
690 Hogg, A. G., Hughen, K. A., Kaiser, K. F., Kromer, B., Manning, S. W., Niu, M., Reimer, R. W., Richards, D. A., Scott,
E. M., Southon, J. R., Staff, R. A., Turney, C. S. M., van der Plicht, J.: IntCal13 and Marine13 Radiocarbon Age
Calibration Curves 0-50,000 years cal BP, *Radiocarbon*, 55, 1869–1887, doi: 10.2458/azu_js_rc.55.16947, 2013.
- Reolid, J., Reolid, M., Betzler, C., Lindhorst, S., Wiesner, M. G., and Lahajnar, N.: Upper Pleistocene cold-water corals
from the Inner Sea of the Maldives: taphonomy and environment, *Facies*, 63:8, doi: 10.1007/s10347-016-0491-7, 1–20,
695 2017.
- Rixen, T., Haake, B., Ittekkot, V., Guptha, M. V. S., Nair, R. R., and Schlüssel, P.: Coupling between SW monsoon-related
surface and deep ocean processes as discerned from continuous particle flux measurements and correlated satellite data,
Journal of Geophysical Research, 101, 28569–28582, doi: 10.1029/96JC02420, 1996.
- Roberts, A. P., Rohling, E. J., Grant, K. M., Larrasoña, J. C., and Liu, Q.: Atmospheric dust variability from Arabia and
700 China over the last 500,000 years, *Quaternary Science Reviews*, 30: 3537–3541, doi: 10.1016/j.quascirev.2011.09.007,
2011.
- Ronge, T. A., Steph, S., Tiedemann, R., Prange, M., Merkel, U., Nürnberg, D., and Kuhn, G.: Pushing the boundaries:
Glacial/interglacial variability of intermediate and deep waters in the southwest Pacific over the last 350,000 years,
Paleoceanography, 30, 23–38, doi: 10.1002/2014PA002727, 2015.
- 705 Rostek, F., Bard, E., Beaufort, L., Sonzogni, C., and Ganssen, G.: Sea surface temperature and productivity records for the
past 240 ka in the Arabian Sea, *Deep-Sea Research II*, 44, 1461–1480, doi: 10.1016/S0967-0645(97)00008-8, 1997.
- Rühlemann, C., Müller, P. J., and Schneider, R. R.: Organic carbon and carbonate as paleoproductivity proxies: Examples
from high and low productivity areas of the tropical Atlantic. In: Fischer, G. and Wefer, G. (Eds), *Use of proxies in
paleoceanography: Examples from the South Atlantic*. Springer, Berlin, Heidelberg, 315–344, 1999.
- 710 Ruth, U., Wagenbach, D., Steffensen, J. P., and Bigler, M.: Continuous record of microparticle concentration and size
distribution in the central Greenland NGRIP ice core during the last glacial period, *Journal of Geophysical Research*,
Atmospheres, 108, 1–12, doi:10.1029/2002JD002376, 2003.
- Sarkar, S. and Gupta, A. K.: Deep-sea paleoceanography of Maldives Islands (ODP Hole 716A), equatorial Indian Ocean
during MIS 12-6, *Journal of Bioscience*, 34, 749–764, doi: 10.1007/s12038-009-0066-7, 2009.



- 715 Sarkar, S. and Gupta, A. K.: Late Quaternary productivity changes in the equatorial Indian Ocean (ODP Hole 716A), *Palaeogeography, Palaeoclimatology, Palaeoecology*, 397, 7–19, doi: 10.1016/j.palaeo.2013.12.002, 2014.
- Sasamal, S. K.: Island wake circulation off Maldives during boreal winter, as visualised with MODIS derived chlorophyll-a data and other satellite measurements, *International Journal of Remote Sensing*, 28, 891–903, doi: 10.1080/01431160600858459, 2007.
- 720 Schmiedl, G., Mackensen, A., and Müller, P. J.: Recent benthic foraminifera from the eastern South Atlantic Ocean: Dependence on food supply and water masses, *Marine Micropaleontology*, 32, 249–287, doi: 10.1016/S0377-8398(97)00023-6, 1997.
- Schmiedl, G. and Leuschner, D. C.: Oxygenation changes in the deep western Arabian Sea during the last 190,000 years: productivity versus deep-water circulation, *Paleoceanography*, 20, PA2008, 1–14, doi: 10.1029/2004PA001044, 2005.
- 725 Schmiedl, G. and Mackensen, A.: Multispecies stable isotopes of benthic foraminifers reveal past changes of organic matter decomposition and deepwater oxygenation in the Arabian Sea, *Paleoceanography*, 21, PA4213, 1–14, doi:10.1029/2006PA001284, 2006.
- Schoepfer, S. D., Shen, J., Wei, H., Tyson, R. V., Ingall, E., and Algeo, T. J.: Total organic carbon, organic phosphorus, and biogenic barium fluxes as proxies for paleomarine productivity, *Earth-Science Reviews*, 149, 23–52, doi: 10.1016/j.earscirev.2014.08.017, 2015.
- 730 Schott, F. A. and McCreary Jr., J. P.: The monsoon circulation of the Indian Ocean, *Progress in Oceanography*, 51, 1–123, doi: 10.1016/S0079-6611(01)00083-0, 2001.
- Schulz, H., von Rad, U., and Erlenkeuser, H.: Correlation between Arabian Sea and Greenland climate oscillation of the past 110,000 years, *Nature*, 393, 54–57, doi: 10.1038/31750, 1998.
- 735 Singh, A. D., Jung, S. J. A., Darling, K., Ganeshram, R., Ivanochko, T., and Kroon, D.: Productivity collapses in the Arabian Sea during glacial cold phases, *Paleoceanography*, 26, PA3210, 1–10, doi:10.1029/2009PA001923, 2011.
- Sirocko, F. and Lange, H.: Clay-mineral accumulation rates in the Arabian Sea during the late Quaternary, *Marine Geology*, 97, 105–119, doi: 10.1016/0025-3227(91)90021-U, 1991.
- Stramma, L., Johnson, G. C., Sprintall, J., and Mohrholz, V.: Expanding oxygen-minimum zones in the tropical oceans, *Science*, 320, 655–658, doi: 10.1126/science.1153847, 2008.
- 740 Stuiver, M. and Reimer, P. J.: Extended ^{14}C data base and revised CALIB 3.0 ^{14}C age calibration program, *Radiocarbon*, 35, 215–230, 1993.
- Sun, X., Corliss, B. H., Brown, C. W., and Showers, W. J.: The effect of primary productivity and seasonality on the distribution of deep-sea benthic foraminifera in the North Atlantic, *Deep-Sea Research I*, 53, 28–47, doi: 10.1016/j.dsr.2005.07.003, 2006.
- 745 Weiss, R. F., Broecker, W. S., Craig, H., and Spencer, D.: GEOSECS Indian Ocean Expedition: Hydrographic Data 1977–1978, 5, U.S. Government Printing Office, Washington, D.C., 1–62, 1983.



- Wiggert, J. D., Murtugudde, R. G., and Christian, J. R.: Annual ecosystem variability in the tropical Indian Ocean: Results of a coupled bio-physical ocean general circulation model, *Deep Sea Research Part II, Topical Studies in Oceanography*, 53, 644–676, doi: 10.1016/j.dsr2.2006.01.027, 2006.
- 750
- Winckler, G., Anderson, R. F., Fleisher, M. Q., McGee, D., and Mahowald, N.: Covariant glacial-interglacial dust fluxes in the equatorial Pacific and Antarctica, *Science*, 320, 93–96, doi: 10.1126/science.1150595, 2008.
- Wyrski, K.: Physical oceanography of the Indian Ocean. In: Zeitzschel, B. and Gerlach, S. A. (Eds.), *The biology of the Indian Ocean*, Springer-Verlag, Berlin, Heidelberg, 18–36, 1973.
- 755
- You, Y.: Intermediate water circulation and ventilation of the Indian Ocean derived from water-mass contributions, *Journal of Marine Research*, 56, 1029–1067, 1998.
- Zhang, X. Y., Arimoto, R., and An, Z. S.: Glacial and interglacial patterns for Asian dust transport, *Quaternary Science Review*, 18, 811–819, doi: 10.1016/S0277-3791(98)00028-6, 1999.
- Zhang, X. Y., Lu, H. Y., Arimoto, R., and Gong, S. L.: Atmospheric dust loadings and their relationship to rapid oscillations of the Asian winter monsoon climate: two 250-ka loess records, *Earth and Planetary Science Letters*, 202, 637–643, doi: 10.1016/S0012-821X(02)00797-5, 2002.
- 760



Table Captions

Table 1: Accelerator Mass Spectrometry (AMS) radiocarbon dating results based on mixed surface-dwelling planktonic foraminifera (*Gr* = *Globigerinoides ruber*, white; *Gs* = *Globigerinoides sacculifer*) from 35 cm, 80 cm and 140 cm sediment depth of core SO-236-052-4. Conventional radiocarbon ages were calibrated using the radiocarbon calibration program CALIB (version 7.0.4; Stuiver and Reimer, 1993) and the calibration curve Marine13 (Reimer et al., 2013).

No.	Sample ID	Lab ID	Material	Core depth [mbsf]	¹³ C/ ¹² C o/oo	¹⁴ C age ya BP	Calibrated age (ΔR 0)		
							cal BP (2s ranges, 95.4 % probability)		
							range [years]	rel. area u. distr.	median of prob. [ka]
1	SO236-052-035	Beta-418574	Gr, Gs	0.35	+1.4	7940 ±30	8330 - 8480	1.00	8.4 ± 0.08
2	SO236-052-080	Beta-418575	Gr, Gs	0.80	+1.6	12890 ±40	14310 - 15020	1.00	14.7 ± 0.36
3	SO236-052-140	Beta-418576	Gr, Gs	1.40	+1.8	23930 ±100	27480 - 27850	1.00	27.7 ± 0.19

770

Table 2: Species composition of benthic foraminiferal assemblages. Principal component number, dominant and important associated species with principal component scores (Q-mode) and explained variance in percent of total variance are given.

Q-mode Principal Components	Species	Scores	Explained variance [%]
PC1	<i>Neouvirgerina proboscidea</i>	5.812	31.54
	<i>Discorbinella araucana</i>	3.948	
	<i>Hyalinea inflata</i>	2.562	
	<i>Cymbaloporeta squamosa</i>	1.913	
	<i>Bulimina marginata</i>	1.729	
	<i>Rosalina vilardeboana</i>	1.595	
PC2	<i>Cibicides mabahethi</i>	7.466	30.54
	<i>Discorbinella bertheloti</i>	1.756	
	<i>Siphogenerina columellaris</i>	1.622	
	<i>Gyroidina umbonata</i>	1.589	
	<i>Reophax</i> sp.	1.387	
	<i>Hyalinea inflata</i>	1.214	
	<i>Discorbinella araucana</i>	1.109	
PC3	<i>Neouvirgerina proboscidea</i>	4.608	27.06
	<i>Hoeglundina elegans</i>	3.952	
	<i>Discorbinella bertheloti</i>	3.004	
	<i>Cibicidoides subhaidingeri</i>	2.311	
	<i>Discorbis</i> sp.	2.161	
	<i>Spiroplectinella sagittula</i> s.l.	1,808	
	<i>Cibicides mabahethi</i>	1,084	

775



Figure Captions

Figure 1: Location maps of the Maldives archipelago in the Indian Ocean (a, b) and the setting of the study area (c) (modified after Betzler et al., 2013a), showing the location of sediment core M74/4-1143 in the Kardiva Channel and core SO-236-052-4 in the central part of the Inner Sea (red circles).

780

Figure 2: Full resolution stable oxygen isotope records of the planktonic foraminifer *G. ruber* (a) and age-depth plots for the sediment cores SO-236-052 (light blue) and M74/4-1143 (grey). Orange triangles indicate radiocarbon dates and circles indicate age control points derived from correlation with the LR04 benthic isotope stack of Lisiecki and Raymo (2005). Sedimentation rates are derived from linear interpolation between age data. MIS denotes the Marine stable oxygen isotope stages.

785

Figure 3: Stable oxygen and carbon isotope records of planktonic and benthic foraminifera of sediment core SO-236-052. Displayed are the planktonic species *G. ruber* (light blue), the epibenthic species *C. mabahethi* (dark blue) and the deep infaunal species *G. affinis* s.l. (red). MIS denotes the Marine stable oxygen isotope stages.

790

Figure 4: Sedimentological and geochemical records of sediment core SO-236-052-4 from the central part of the Maldives Inner Sea. a) Sortable silt (black) and bulk sediment (grey) MEAN values, b) Total Organic Carbon (TOC) (dark green) and calcium carbonate (light green) content of the sediment, c) iron (dark blue) and silicium (light blue), and d) barium (pink) and strontium (purple). All element count rates are given in relation to the calcium counts of the XRF core scans. Thin lines represent full-resolution data, bold lines indicate five-point running averages. Only the Ba/Ca ratio is displayed with a fifteen-point running average. MIS denotes the Marine stable oxygen isotope stages.

795

Figure 5: a) Epibenthic stable oxygen isotope record of core SO-236-052-4 (dark blue) in comparison with the LR04 benthic stable isotope stack (dashed grey line; Lisiecki and Raymo 2005). b-c) Comparison of the sortable silt records of sediment cores M74/4-1143 and SO-236-052-4, and d) relative abundance of meroplanktonic Benthic Foraminifera (BF; including the genera *Cymbaloporeta* and *Tretomphaloides*) in sediments of core SO-236-052-4. Thin lines represent full-resolution data, bold lines indicate five-point running averages. MIS denotes the Marine stable oxygen isotope stages.

800

Figure 6: Comparison of benthic foraminiferal faunal records of core SO-236-052-4 from the central part of the Maldives Inner Sea. a) Shannon-Wiener diversity index $H(S)$, b-d) Q-mode benthic foraminiferal assemblages, including the *N. proboscidea*-*D. araucana*-fauna (assemblage 1), the *C. mabahethi*-fauna (assemblage 2), and the *N. proboscidea*-*H. elegans*-fauna (assemblage 3). Loadings ≥ 0.5 are defined as significant after Backhaus et al. (2008). e-g) Distribution of

805



selected important and associated benthic foraminiferal taxa, given in percent. The meroplanktonic Benthic Foraminifera (BF) comprise the genera *Cymbaloporeta* and *Tretomphaloides*.

810

Figure 7: Variation of the insolation difference between the June and December solstice at 30° N (after Laskar, 2004; calculated with AnalySeries 2.0: Paillard et al. 1996) (a) in comparison with geochemical and benthic foraminiferal productivity records of core SO-236-052-4. b) Total Organic Carbon (TOC) content and c) Ba/Ca ratio as derived from XRF scanning count rates as indicator for surface water productivity. d) Fe/Ca ratio and e) relative abundance of agglutinated benthic foraminifera as indicator for enhanced dust supply. f) Principal Components (PC) show the *C. mabahethi*-fauna (assemblage 2) and *N. proboscidea*-*H. elegans*-fauna (assemblage 3). Thin lines represent full-resolution data, bold lines in b), d) and e) indicate five-point running averages, the bold line in c) indicate a fifteen-point running average. MIS denotes the Marine stable oxygen isotope stages.

815

820

Figure 8: Water mass circulation changes obtained from stable $\delta^{13}\text{C}$ data of core SO-236-052-4 (Indian Ocean) in comparison to ventilation changes in the Arabian Sea. a) $\delta^{13}\text{C}$ records of the planktonic *G. ruber* (light blue) and the epibenthic *C. mabahethi* (dark blue), b) difference between the planktonic and epibenthic stable carbon records ($\Delta\delta^{13}\text{C}_{Gr-Cm}$), c) differences between epibenthic and deep endobenthic $\delta^{13}\text{C}$ records of SO-236-052-4 (dark blue) from the intermediate Maldives Inner Sea in comparison to that of GeoB3004 (purple) from the deep Arabian Sea (Schmiedl and Mackensen, 2006). Changes in intermediate- and deep-water oxygen concentrations are calculated by the linear regression between the $\Delta\delta^{13}\text{C}$ and $\text{O}_2 < 235 \mu\text{mol kg}^{-1}$ after Hoogakker et al. (2015). Variation of the insolation difference between the June and December solstice at 30° N (yellow) were estimated after Laskar (2004) with AnalySeries 2.0 (Paillard et al., 1996). All lines indicate five-point running averages. MIS denotes the Marine stable oxygen isotope stages. *Cib.* = *Cibicides*, *Cm* = *Cibicides mabahethi*, *Cw* = *Cibicides wuellerstorfi*, *Ga* = *Globobulimina affinis*, *Gr* = *Globigerinoides ruber*.

825



830 Figure 1

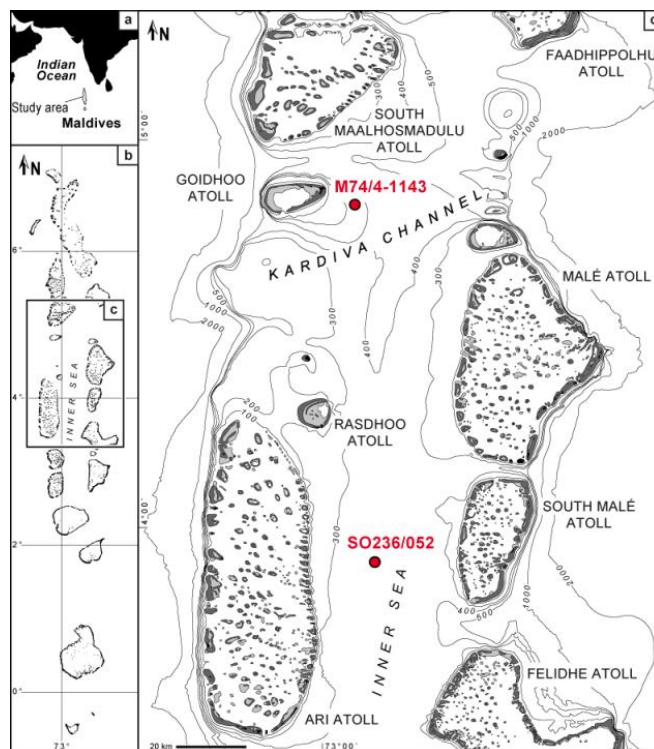




Figure 2

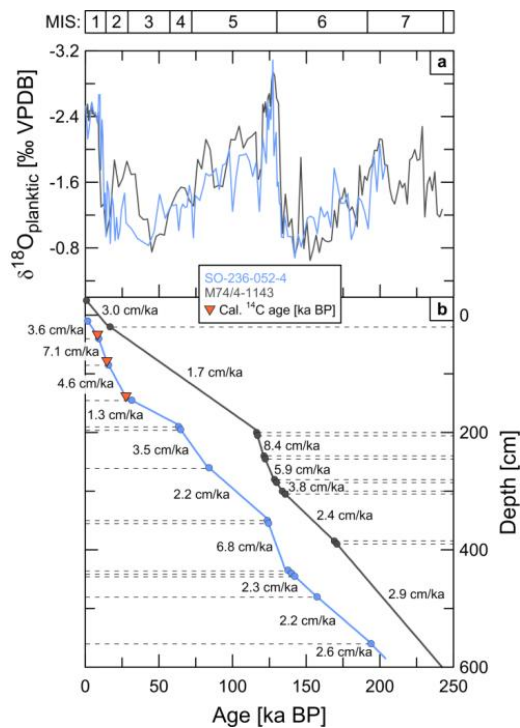




Figure 3

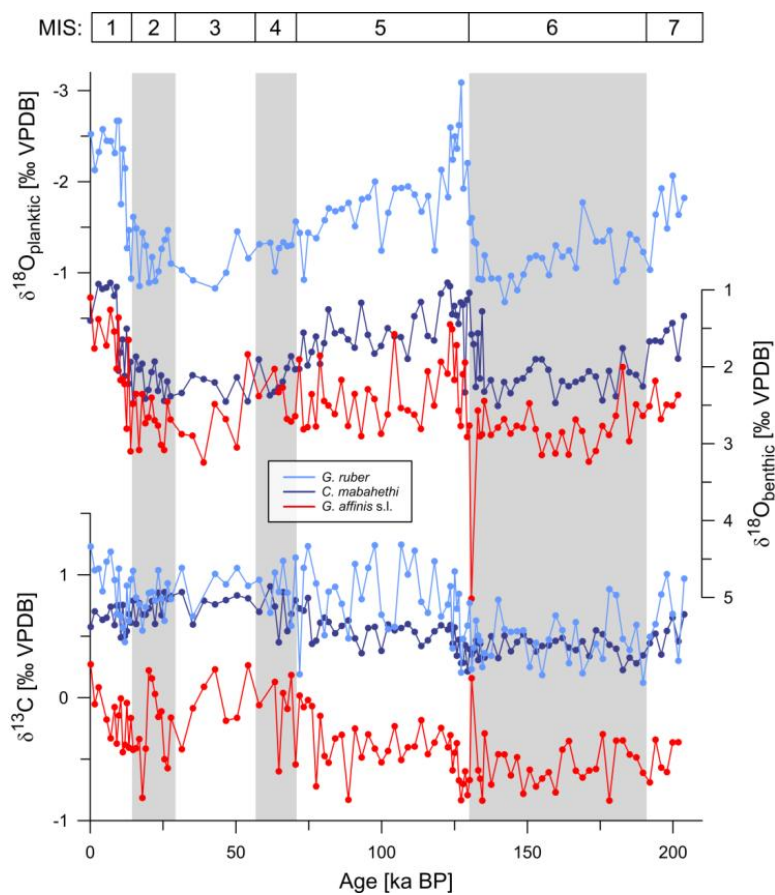




Figure 4

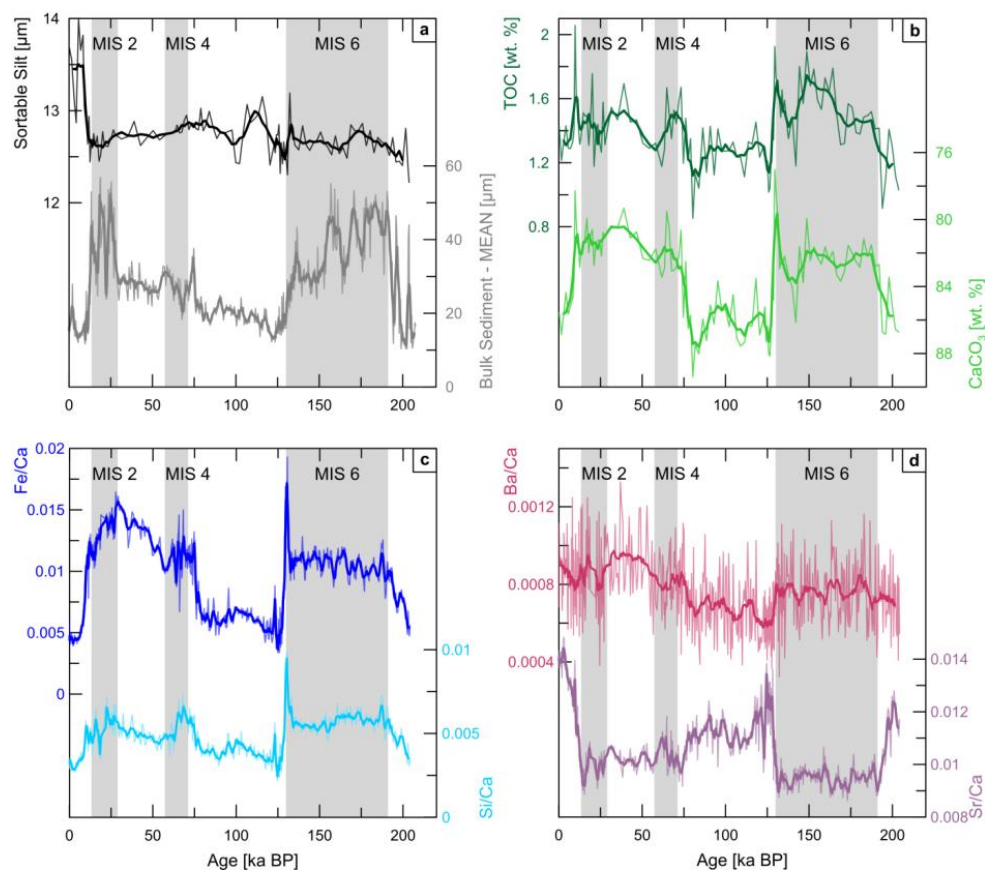
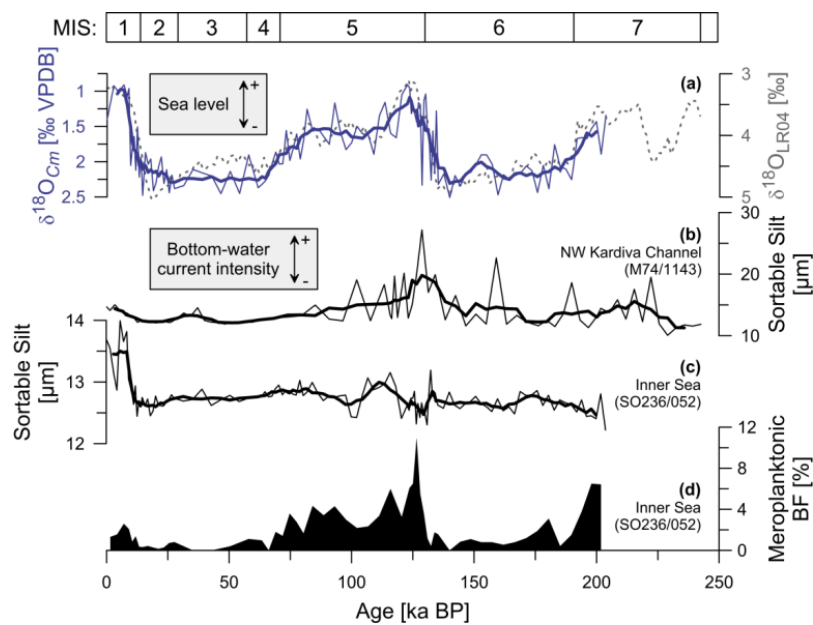




Figure 5





835 Figure 6

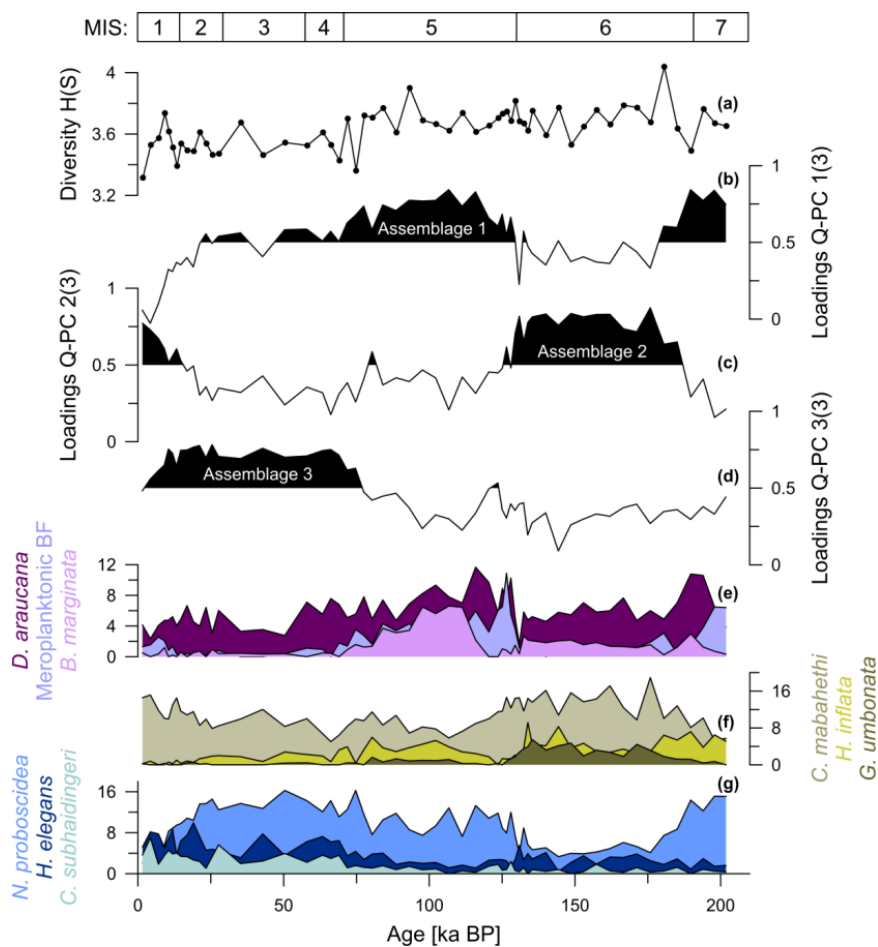




Figure 7

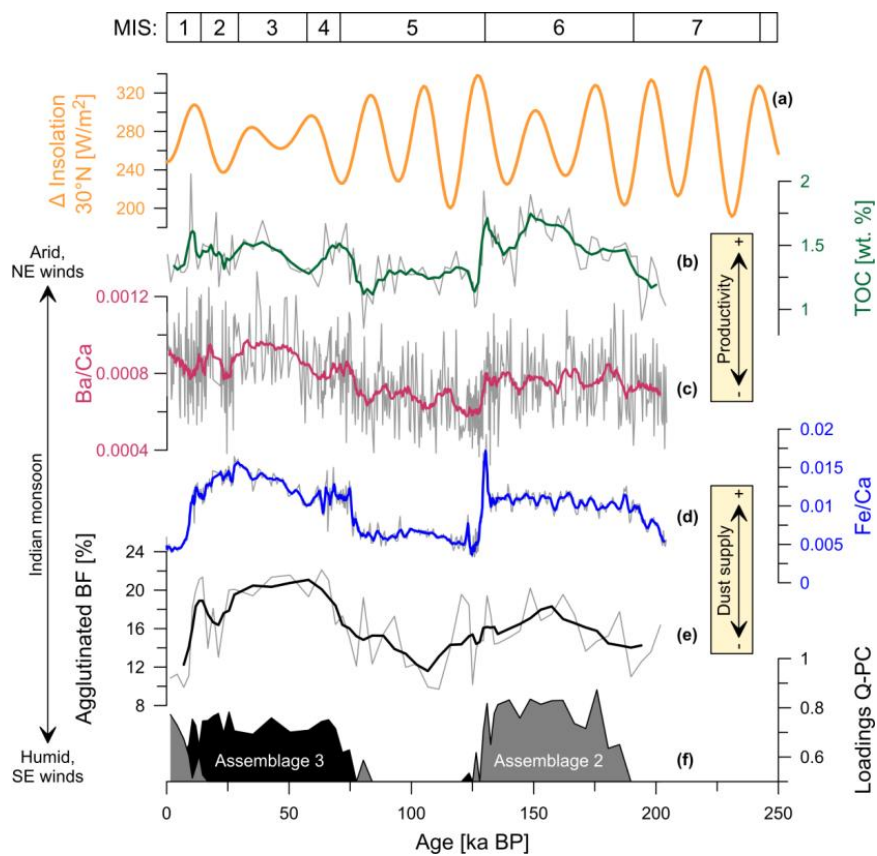




Figure 8

